

LASER REMOTE SENSING

PART I

*Eduardo
Landulfo*

elandulf@ipen.br



<https://www.youtube.com/watch?v=SaBLaLnRm24>



SOME HISTORY...

How the Laser Happened

ADVENTURES OF A SCIENTIST

Charles H. Townes

Some of my colleagues warned me in various ways, "Don't go down there. Stay and build the laser. That is the work that will get you the Nobel Prize." I thought the maser and laser might, in fact, win a Nobel. But, I felt it did not really matter who actually built the first one. The ideas were there. I was not going to make a career decision to go all-out to build one just to win the prize.

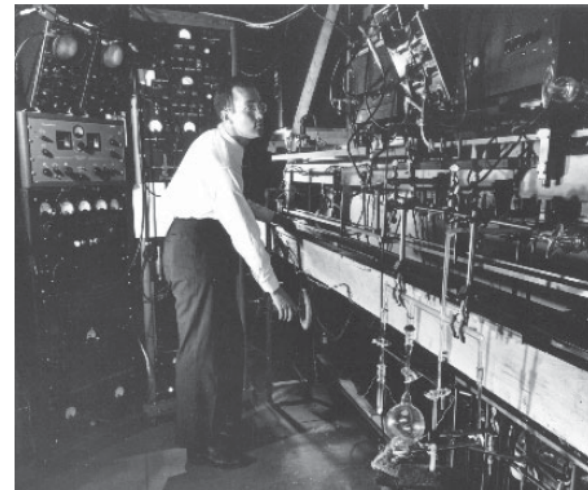


Figure 7. My apparatus for measuring microwave spectra of molecules, built with my students at Columbia University, 1949.



SOME HISTORY...

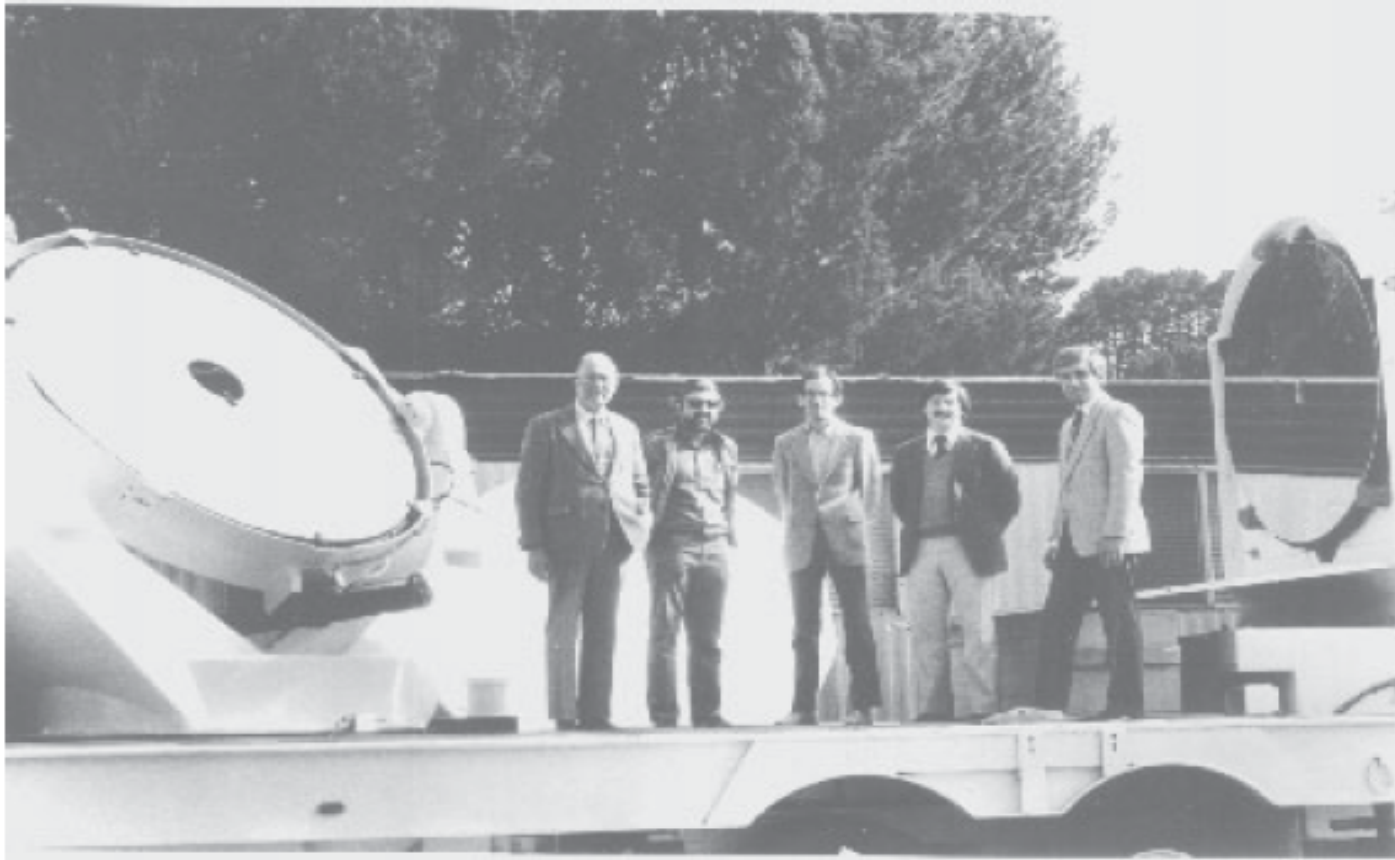
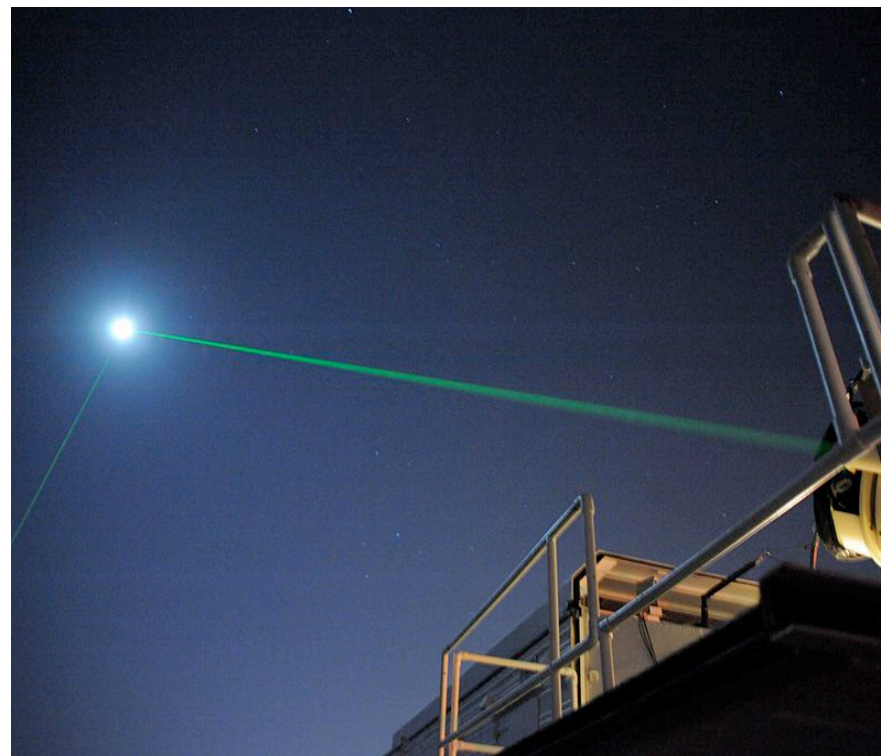
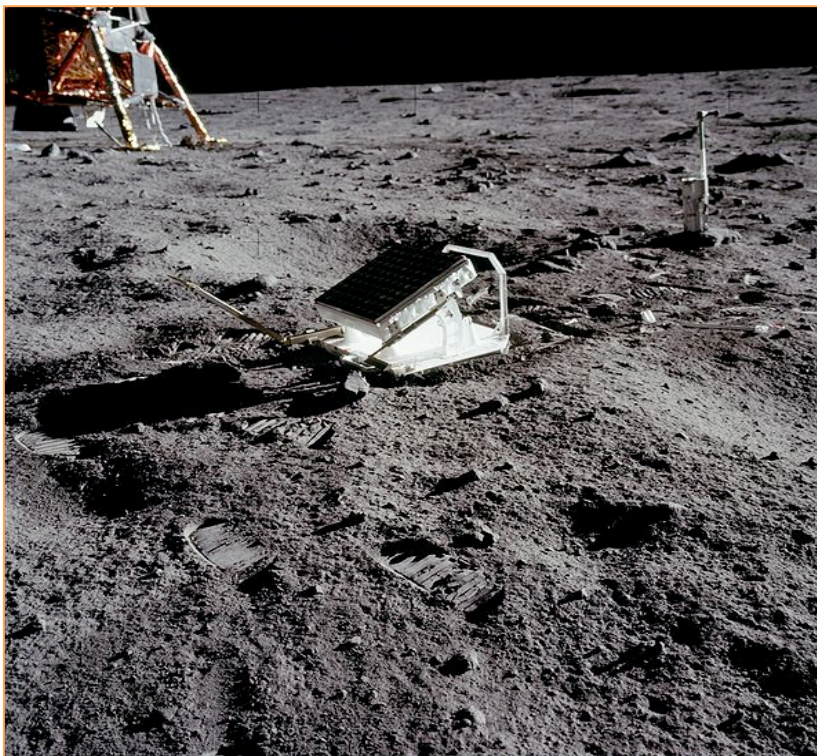


Figure 16. The christening at the University of California of our first large movable telescope on a trailer, one unit of the Infrared Spatial Interferometer, which maps the details of stellar shapes and the clouds around stars. In operation, laser beams shine back and forth between the two mirrors. Left to right are Charles Townes, electronics technician Walter Fitelson, and physicists Edmund Sutton, William Danchi, and Manfred Bester.



TWO BASIC QUESTIONS:



WHAT'S THE DISTANCE BETWEEN THE MOON AND THE EARTH?

HOW MUCH "MATTER" IS BETWEEN THE TWO ?



NON-COHERENT APPROACHES

1930 Syngé proposed a method to determine the atmospheric density with an anti-aircraft searchlight and a telescope (bistatic configuration)

1936 First reported results of density profiles: **Duclaux** (3.4 km), **Hulbert** (28 km)

1938 First reported use of a **monostatic configuration for cloud base height, using a pulsed light source** (Bureau)



1953 First retrieval of temperature profiles from density profiles (**Elterman**)



HOMEWORK: TRY DOING AT HOME...

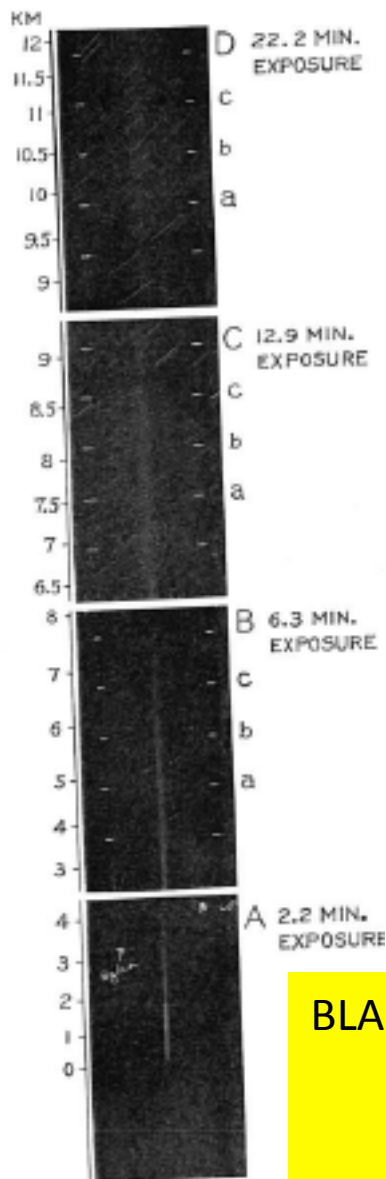


FIG. 1. Photographs of searchlight beams.

BLACK BODY AT 1719 K

BLUE FILTER

655 nm

Inverse square law

$$\frac{d\sigma_e}{d\Omega} = \frac{8\pi}{3} \cdot \frac{\pi^2(n^2 - 1)^2}{N^2\lambda^4} (\cos^2\theta \cos^2\phi + \sin^2\theta)$$

RAYLEIGH SCATTERING

It is difficult to estimate the possible errors in the numbers of columns (3) and (4), Table I; they, and those of column (5), may be correct within a factor of 2. With this qualification the theoretical intensities of column (4) deviate in a regular manner from the observed intensities of column (3) as shown by the ratios of column (5). The ratios decrease from about 7 at 5 km to unity at 10 or 15 km. The deviations would be

⁵ Humphreys, *Physics of the Air* (1929), p. 74.

APPENDIX 1

Photographic determination of the intensity of the beam

A ribbon filament tungsten lamp, standardized by the National Bureau of Standards, burning at a red ($\lambda 0.655\mu$) black body apparent temperature of 1719°K, served as a known source of energy. A diaphragm limited the exposed area of the filament to 0.124 cm². A selected blue filter of known transmission was placed in front of the lamp; the spectral energy curve of the light through the filter is given in curve 1, Fig. 3. The calculated spectral energy curve of the scattered light of the searchlight beam is

TABLE II. Average temperature and density of the atmosphere.

ALTITUDE	TEMP.	DENSITY d	n	ALTITUDE	TEMP.	DENSITY d	n
0 km	1.72°C	1256×10^{-6}	261×10^{17}	20 km	-55°C	89.7×10^{-6}	18.6×10^{17}
2	-4.16	1010	210	22	-55	65.8	13.7
4	-15.3	817	170	24	-55	48.2	10.0
6	-29.3	660	137	26	-55	35.3	7.32
8	-43.6	529	110	28	-55	25.9	5.39
10	-54.2	414	86.0	30	-55	19.0	3.95
12	-55	311	64.5	32	-55	13.9	2.89
14	-55	228	47.5	34	-55	10.2	2.12
16	-55	167	34.7	36	-55	7.54	1.57
18	-55	121	25.2	38	-55	5.53	1.15



ALMOST 30 YEARS LATER...

Light Detection And Ranging

551.501.71 : 551.508.93 : 538.8

Lidar : a new atmospheric probe

By R. T. H. COLLIS
Stanford Research Institute, Menlo Park, California

(Manuscript received 26 July 1965; in revised form 6 December 1965)

PERHAPS THE FIRST
TIME THE WORD (ACRONYM)
LIDAR *was used*

SUMMARY

Pulsed-light techniques of probing the atmosphere have been greatly extended by employing lasers as energy sources in instruments called 'lidars.' Because of the nature of laser energy and the manner in which it is used in current and proposed systems, lidar is best discussed in terms of radar. Apart from the basic capabilities of lidar for detecting backscattering from atmospheric constituents, possibilities exist for more sophisticated techniques based on the wave nature of the energy. The basic capabilities of lidar, however, make it possible to observe the atmosphere with previously unknown resolution and sensitivity. Apart from providing new information about clouds, lidar has shown that the concentration of the particulate matter content of clear air is highly variable and that such variations can indicate the structure and motion of the clear atmosphere. These capabilities have applications in atmospheric and meteorological research and various operational activities.

LIDAR : A NEW ATMOSPHERIC PROBE

223

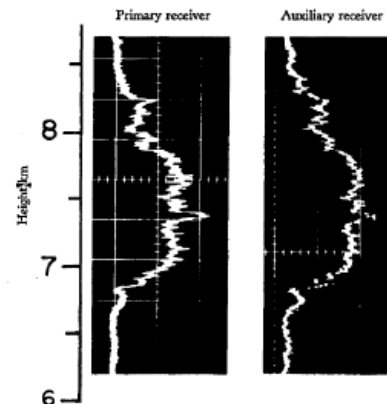
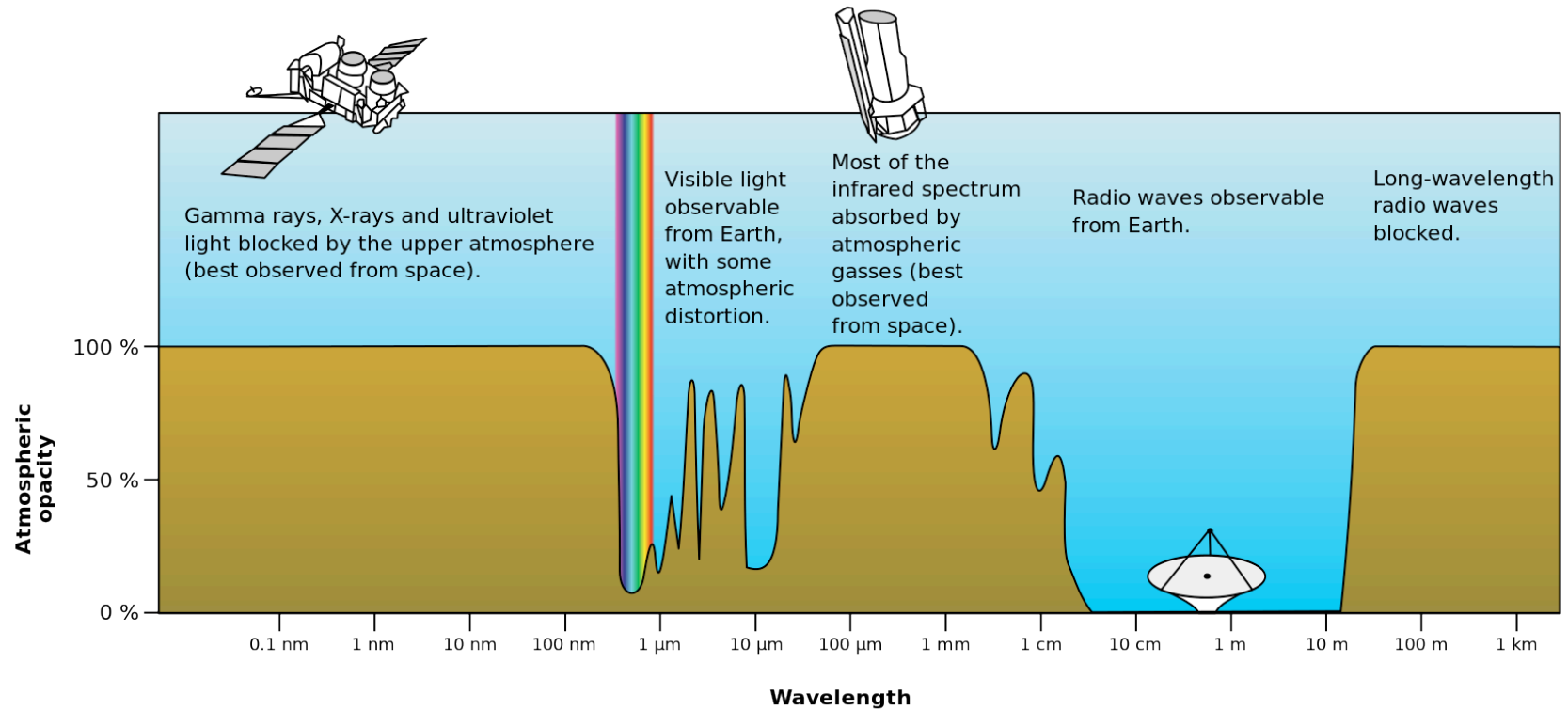


Figure 1. Simultaneous observations of cirrus cloud 4 October 1965. The two traces show the returns (relative intensity vs height) from cirrus cloud as observed simultaneously by the SRI Mark II 1965 lidar and an auxiliary receiver located at a distance of 17 m.

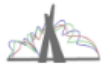
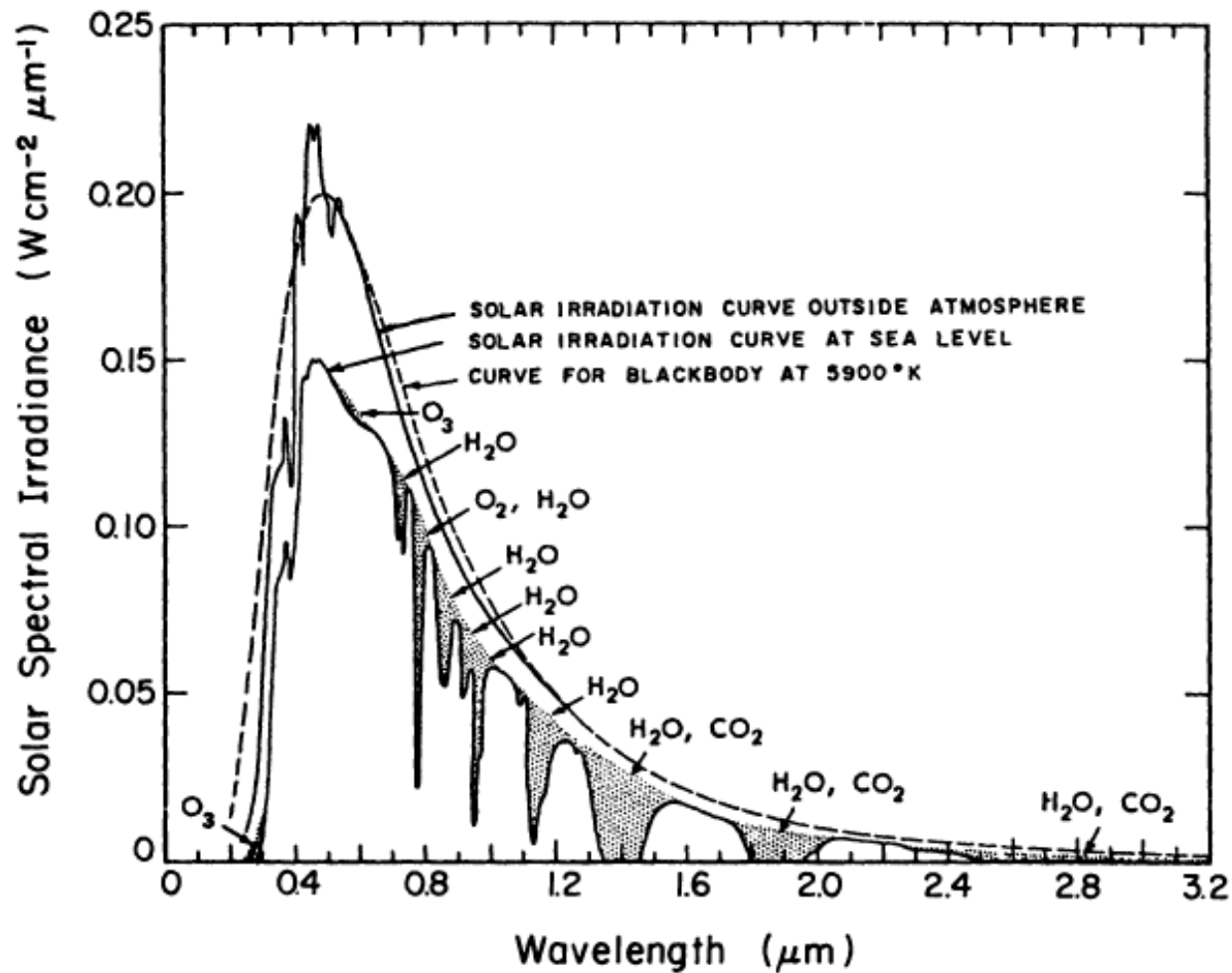
R.T. H. Collins, Lidar: A new atmospheric probe,
Quart. J. Royal Meteor. Society, 220-230, 1966

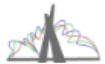
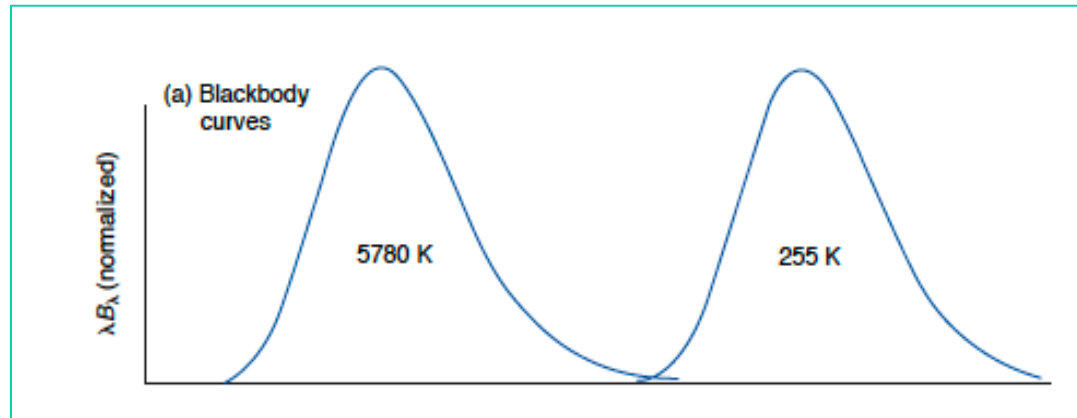
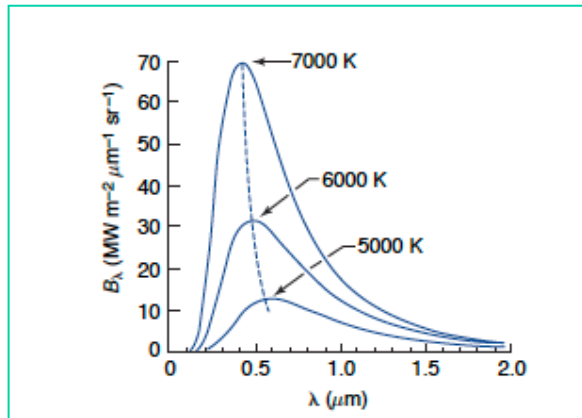
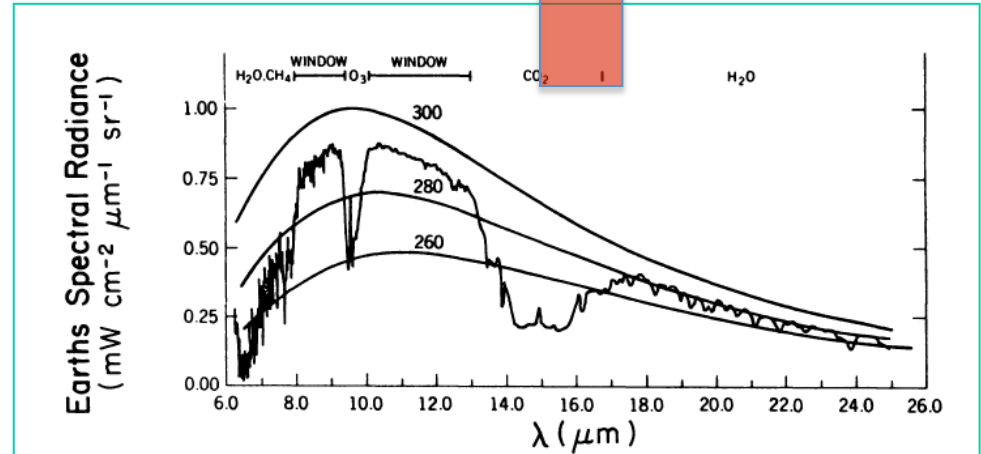
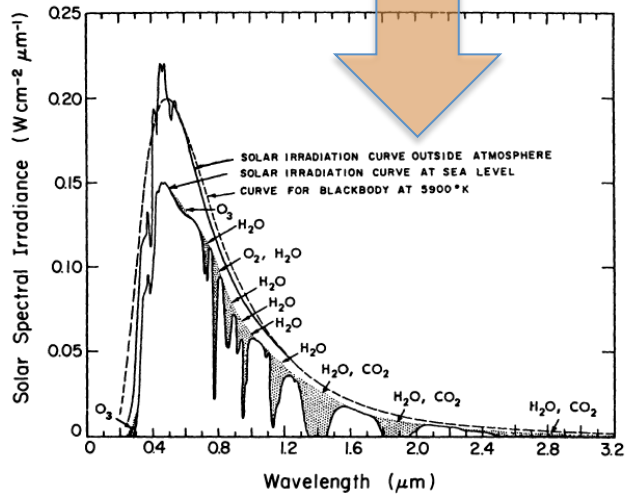


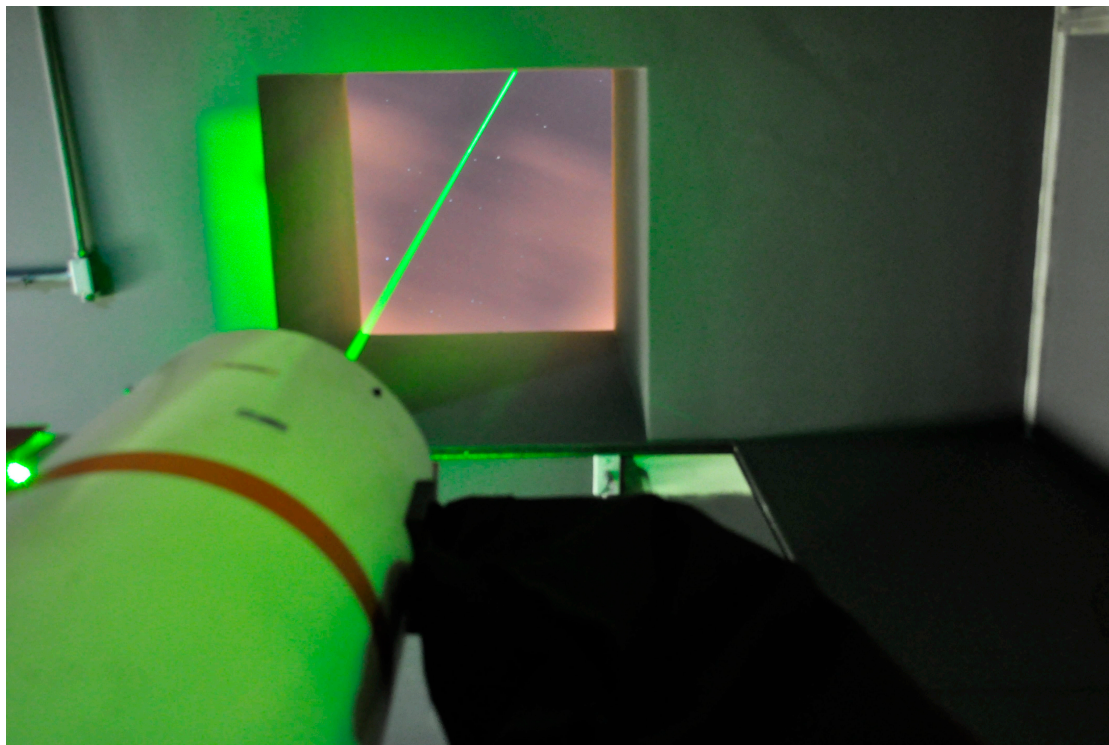
ATMOSPHERIC WINDOW



ATMOSPHERIC WINDOW



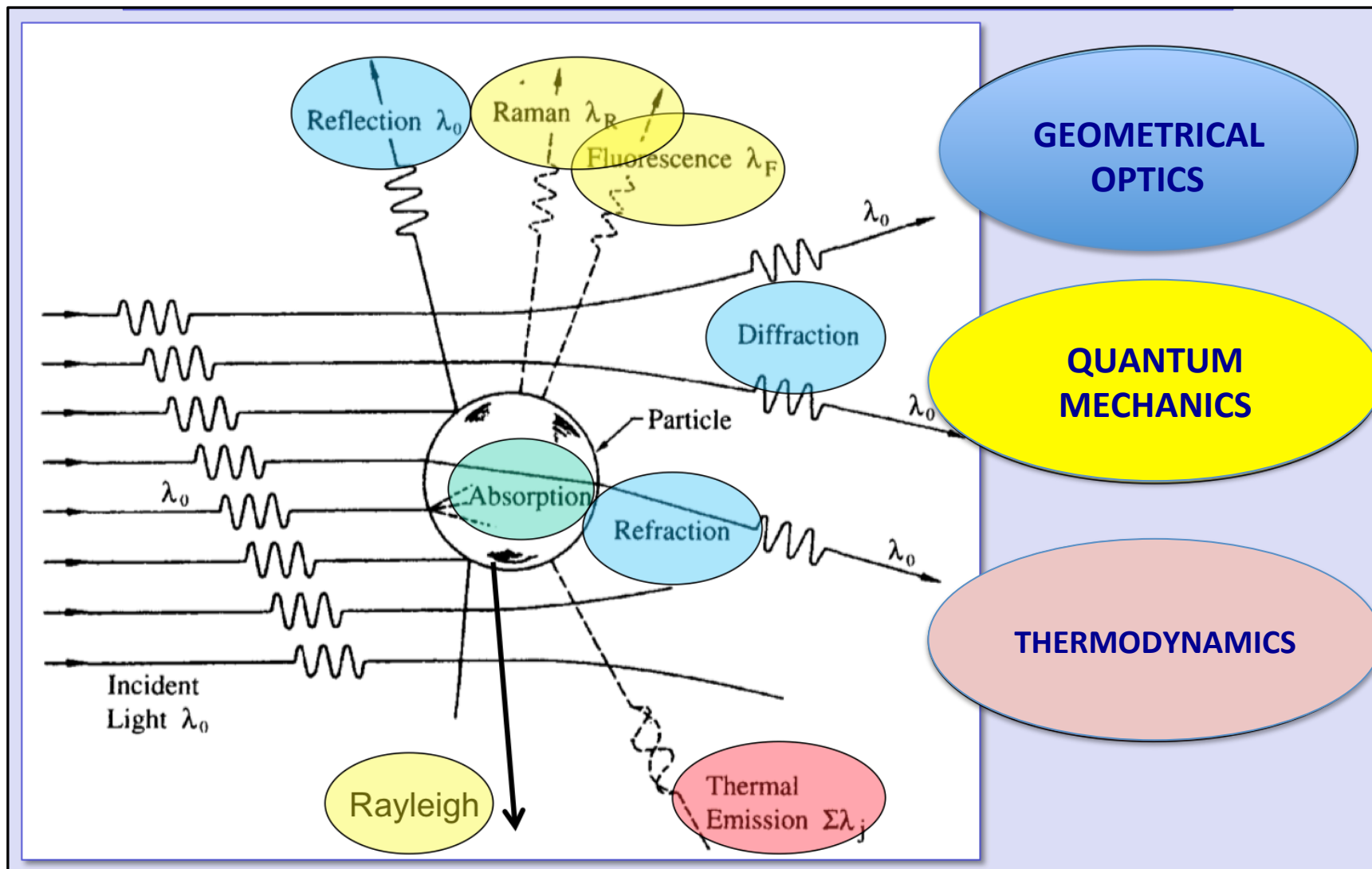




WHAT HAPPENS WHEN ONE SENDS A LASER BEAM INTO THE ATMOSPHERE ?



THE SCATTERING MECHANISMS...



Scattering type	Cross section (cm ²)	Ratio (%)
Rayleigh	1.156×10^{-27}	100
O ₂ RRS	7.10×10^{-29}	6.1
N ₂ RRS	2.94×10^{-29}	2.5
Air RRS	3.82×10^{-29}	3.3
VRS	—	0.1

RAYLEIGH SCATTERING – INTENSITY

The Intensity of the scattered light is proportional to the inverse of the fourth power of the EM wavelength.

$$I_{\lambda} \sim 1/\lambda^4.$$



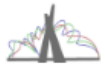
BLUE vs GREEN

$$\frac{\lambda_1}{\lambda_2} = (440 / 550)^4$$

$$\frac{256}{625}$$

‰ // N

0.4096



A LITTLE BIT OF DIMENSIONAL ANALYSIS

$$E_s \propto \frac{E_i V}{r.k}$$

$$[k] = \frac{[E_i][V]}{[r][E_s]}$$

$$[k] = [L]^2$$



$$k = [\lambda]^2$$



A LITTLE BIT MORE OF DIMENSIONAL ANALISYS

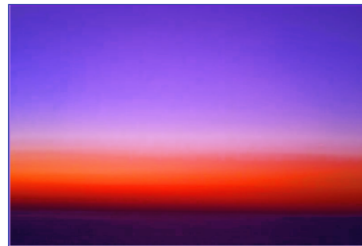
RAYLEIGH SCATTERING – DIMENSION ANALYSIS

SCATTERED INTENSITY (POWER)

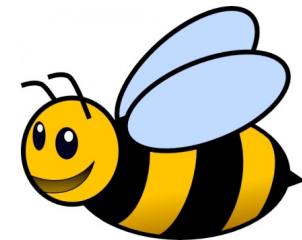
$$I_s \propto E_s^2$$

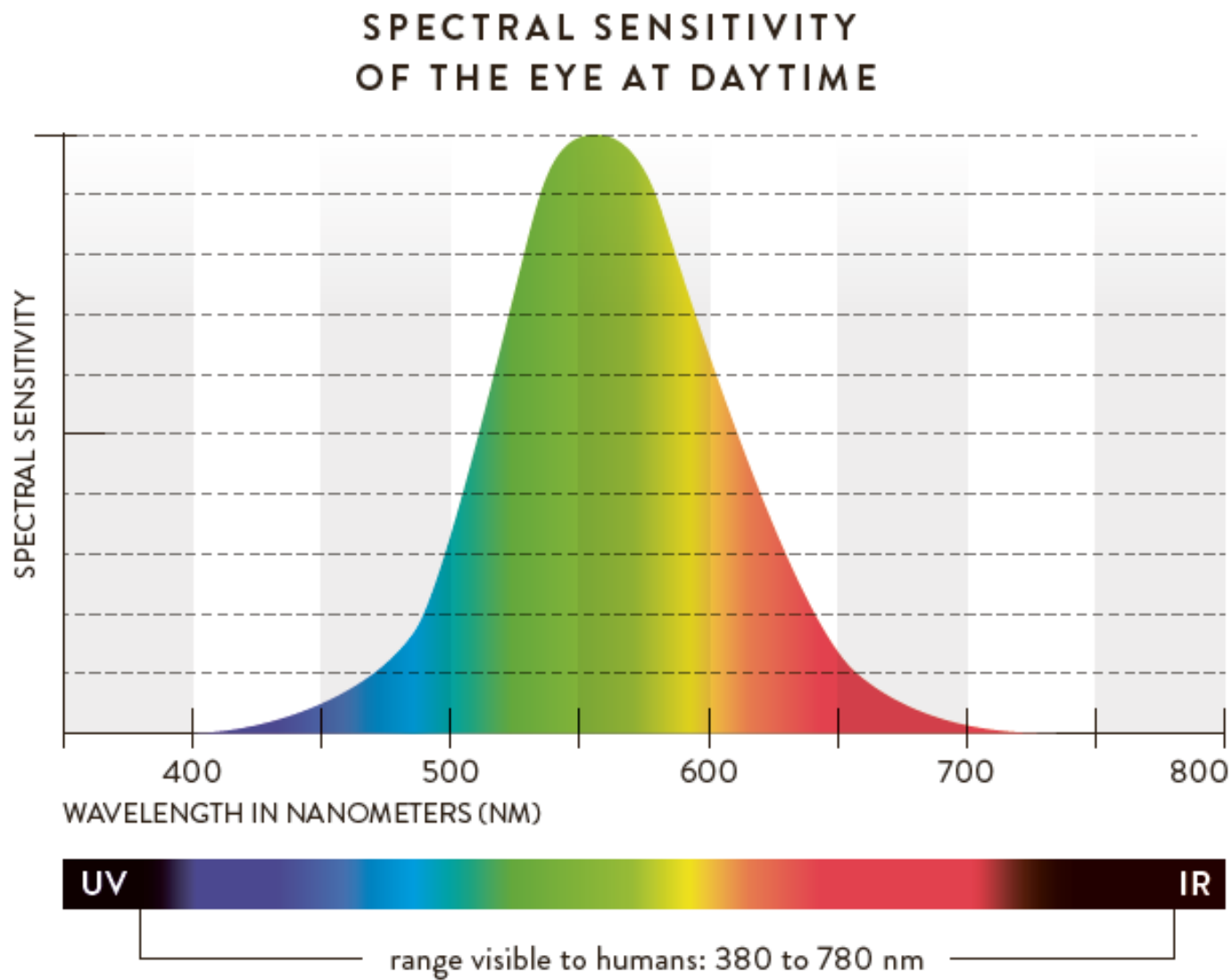
$$I_s \propto \frac{E_i^2 V^2}{r^2 \lambda^4}$$

WHY DON'T WE SEE THE SKY AS VIOLET THEN ?



*“ The wonders of Photoshop
and Gimp ”*

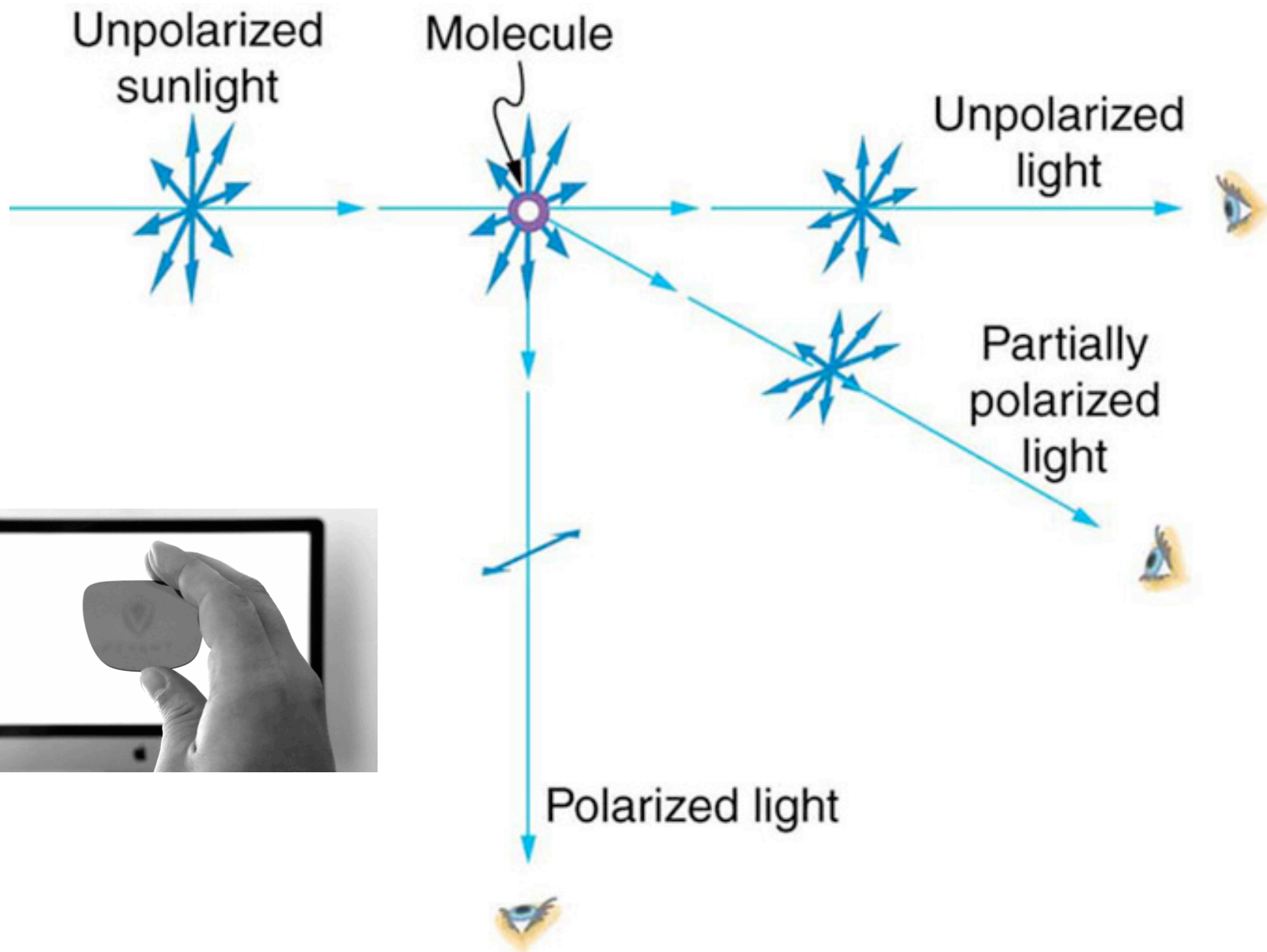




RAYLEIGH SCATTERING CROSS SECTION

$$\sigma_s = \frac{8\pi^3 (m_r^2 - 1)^2}{3\lambda^4 N_s^2} \left(\frac{6 + 3\delta_p}{6 - 7\delta_p} \right)$$

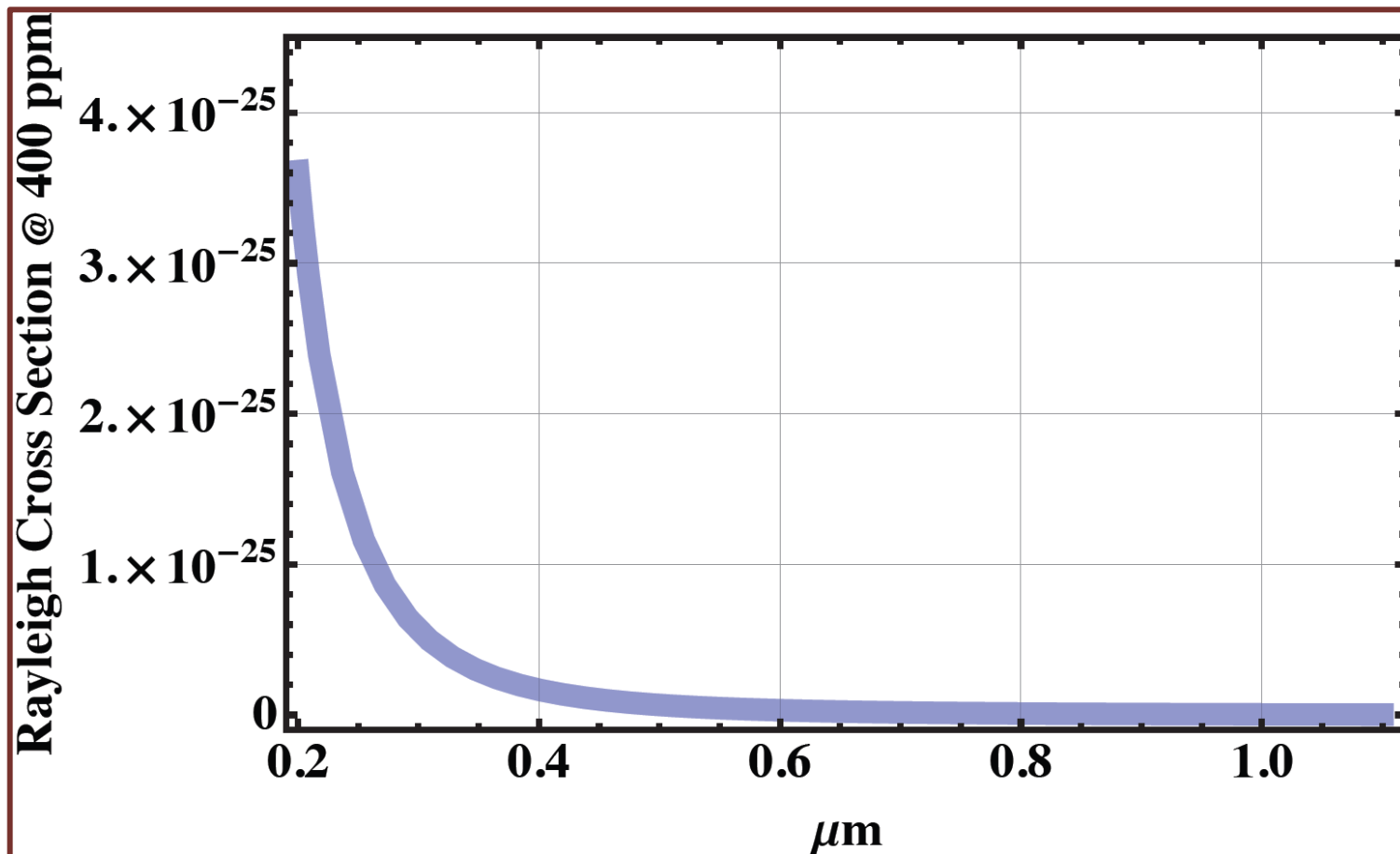


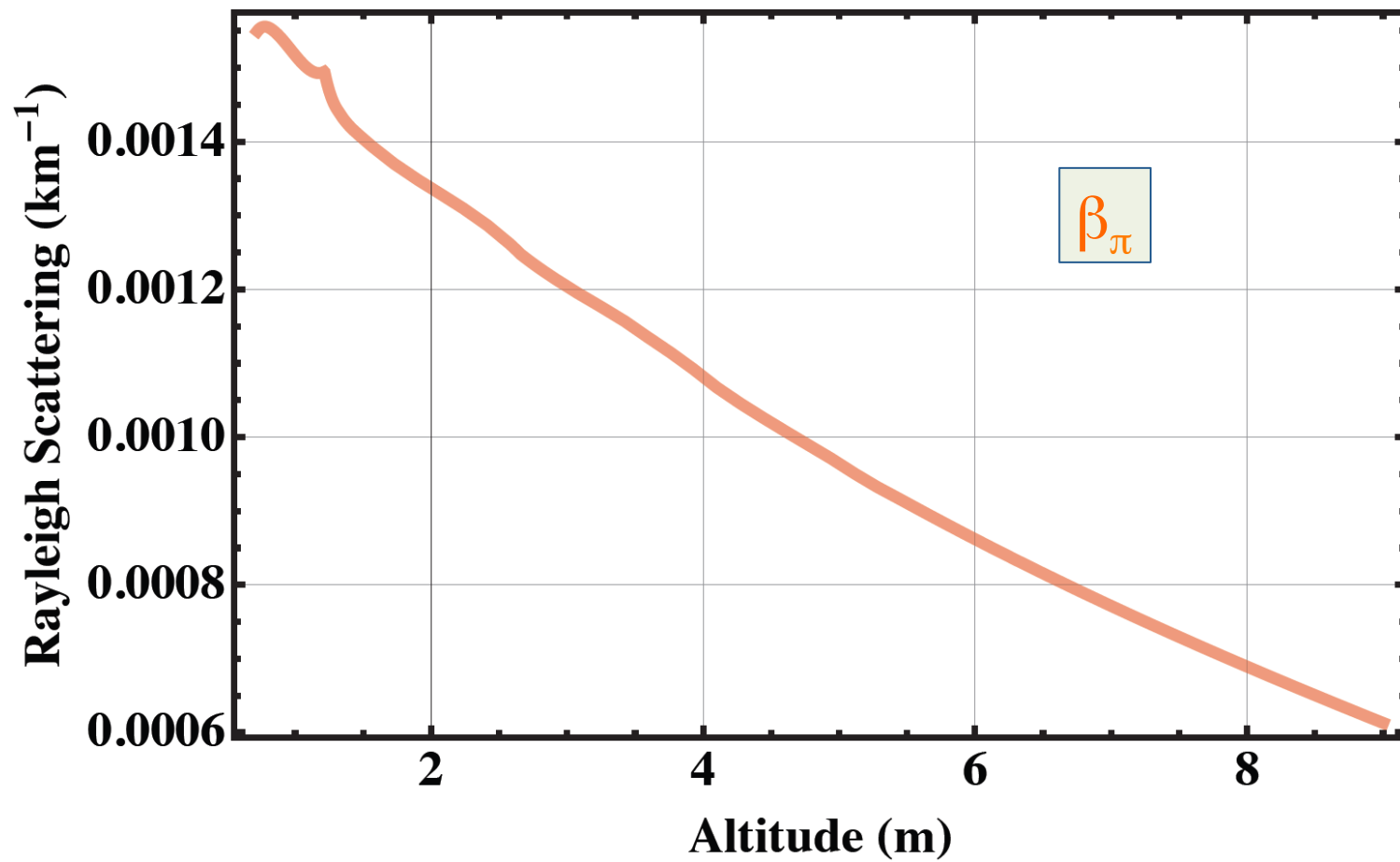


IN SEARCH OF ACCURACY

Here we suggest a method for calculation of Rayleigh optical depth that goes back to first principles as suggested by Penndorf (1957) rather than using curve-fitting techniques, although it is true that the refractive index of air is still derived from a curve fit to experimental data. We suggest using all of the latest values of the physical constants of nature, and we suggest including the variability in refractive index, and also the mean molecular weight of air, due to CO_2 even though these effects are in the range of 0.1%–0.01%. It should be noted that aerosol optical depths are often as low as 0.01 at Mauna Loa. Since Rayleigh optical depth is of the order of 1 at 300 nm, it is seen that a 0.1% error in Rayleigh optical depth translates into a 10% error in aerosol optical depth. Furthermore, it simply makes sense to perform the calculations as accurately as possible.







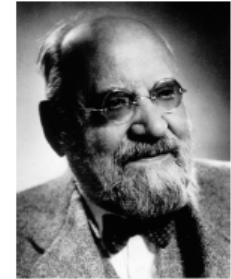
MIE SCATTERING – TOWARDS A BIGGER SCATTERER



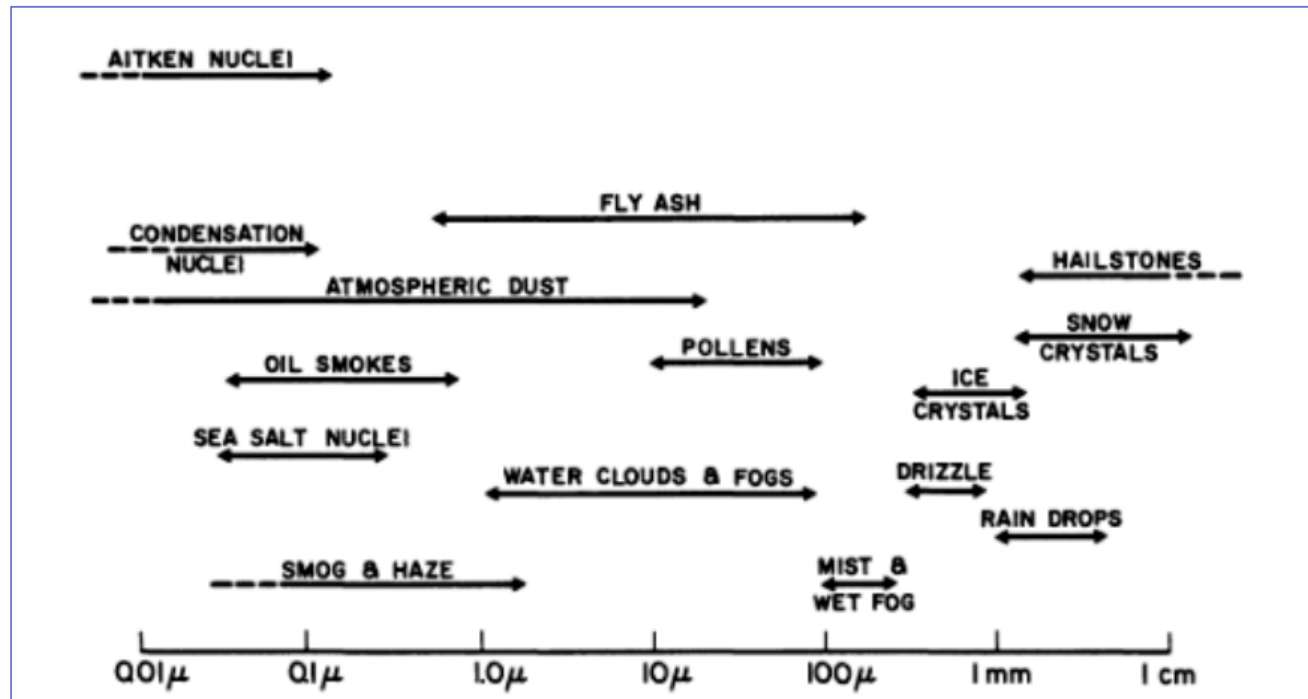
RAYLEIGH



MIE



Gustav Mie (29.09.1868 - 13.02.1957)
Professor in Halle 1917-1924



MIE SCATTERING - BUILDING CONCEPTS

SIZE PARAMETER

$$x = \frac{2\pi a}{\lambda}$$

SCATTERING EFFICIENCY

$$Q_s = \frac{\sigma_s}{\pi \cdot a^2}$$



BOTH ADIMENSIONAL QUANTITIES



MIE SCATTERING – TOWARDS A BIGGER SCATTERER

$$x \ll 1$$

RAYLEIGH SCATTERING

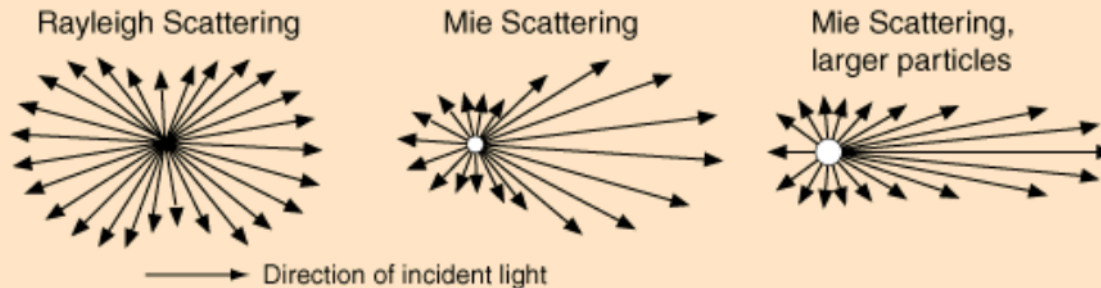
$$x \gtrsim 1$$

MIE SCATTERING



Mie Scattering

The scattering from molecules and very tiny particles ($< 1/10$ wavelength) is predominantly [Rayleigh](#) scattering. For particle sizes larger than a wavelength, Mie scattering predominates. This scattering produces a pattern like an antenna lobe, with a sharper and more intense forward lobe for larger particles.

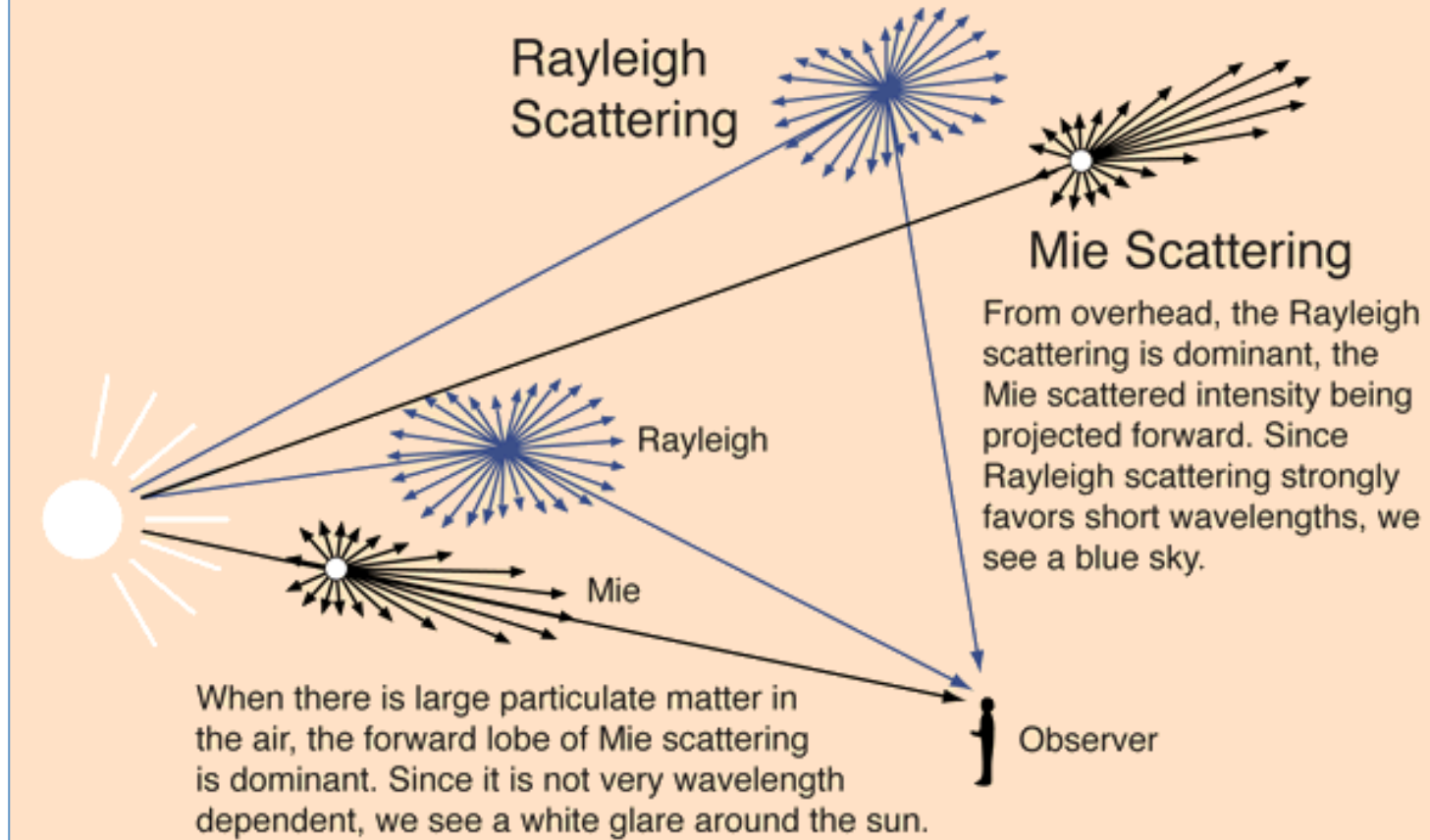


Mie scattering is not strongly wavelength dependent and produces the almost white glare around the sun when a lot of particulate material is present in the air. It also gives us the white light from mist and fog.

[Greenler](#) in his "Rainbows, Haloes and Glories" has some excellent color plates demonstrating Mie scattering and its dramatic absence in the particle-free air of the polar regions.



Rayleigh and Mie Scattering

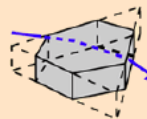




Halos

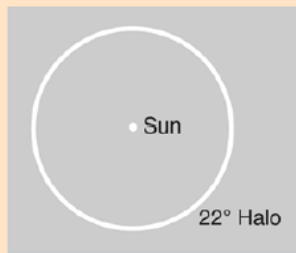
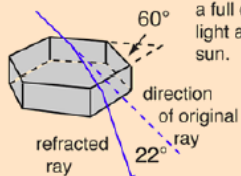
The 22° Halo

The familiar 22° halo around the Sun or Moon occurs because of [refraction](#) in tiny hexagonal ice crystals in the air. With the 60° apex angle of the [prism](#) formed by extending the sides of the crystal and the [index of refraction](#) of ice ($n=1.31$) one can calculate the [angle of minimum deviation](#) to be 21.84°.



Hexagonal ice crystals can be viewed as part of an equilateral 60° prism.

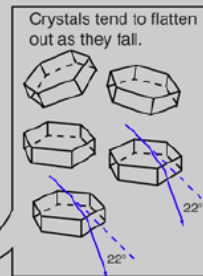
Ice crystals at all orientations in the sky give a full circle of light around the sun.



Sun Dogs

Sun Dogs (Parhelia)

The high intensity spots of light at the horizontal points of the 22° halo compared to the rest of the halo are attributed to the orientation of the falling ice crystals. A portion of the ice crystals are flat hexagonal plates and they tend to orient themselves with flat side horizontal when falling through the air.



MIE SCATTERING – TOWARDS A BIGGER SCATTERER

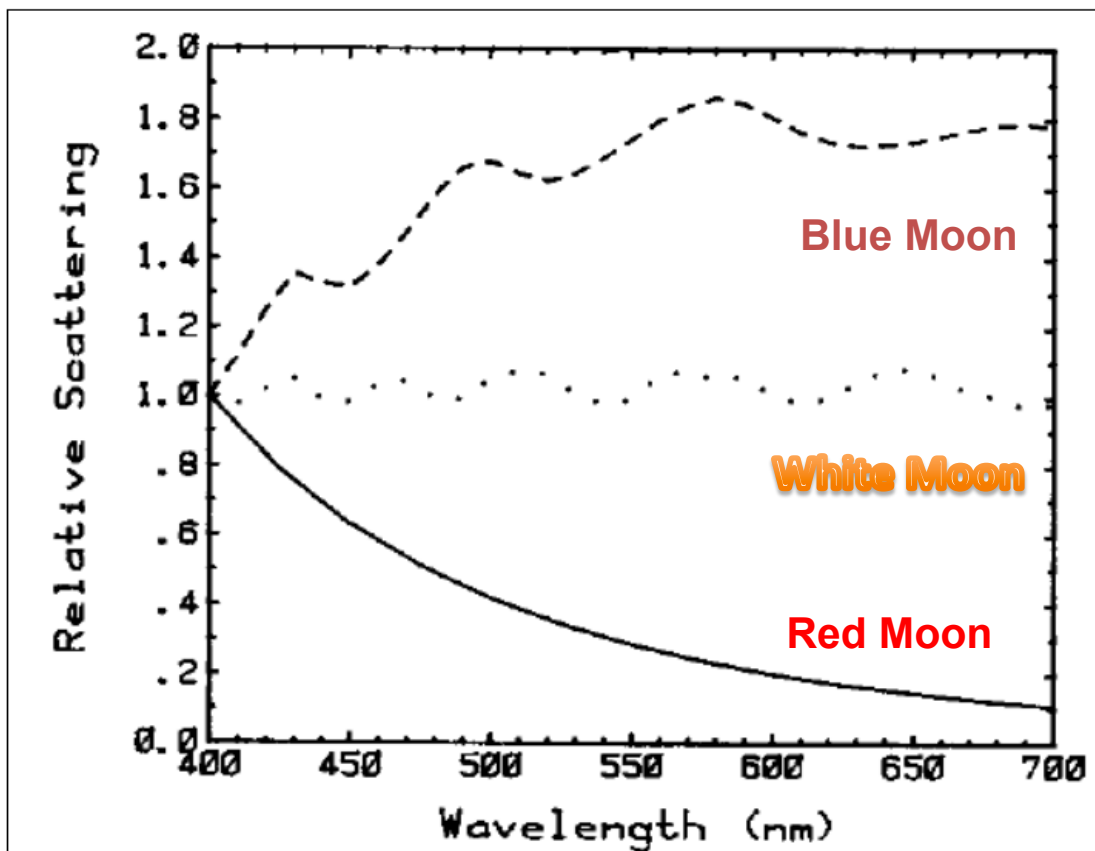
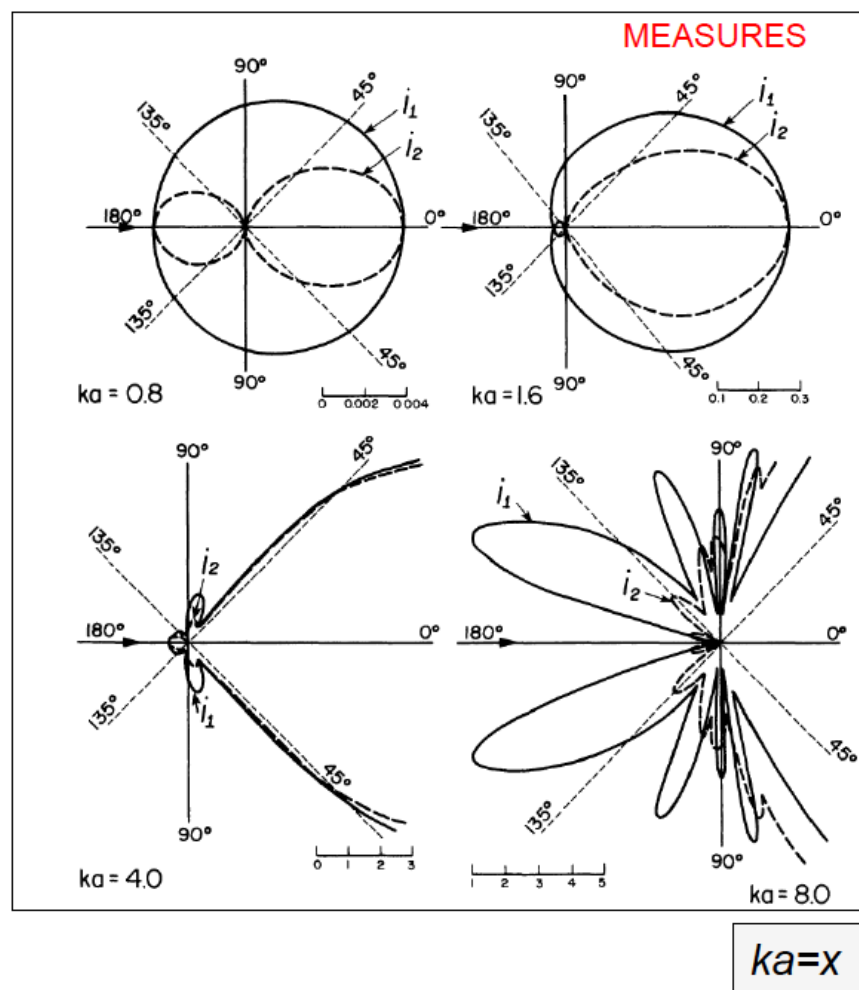
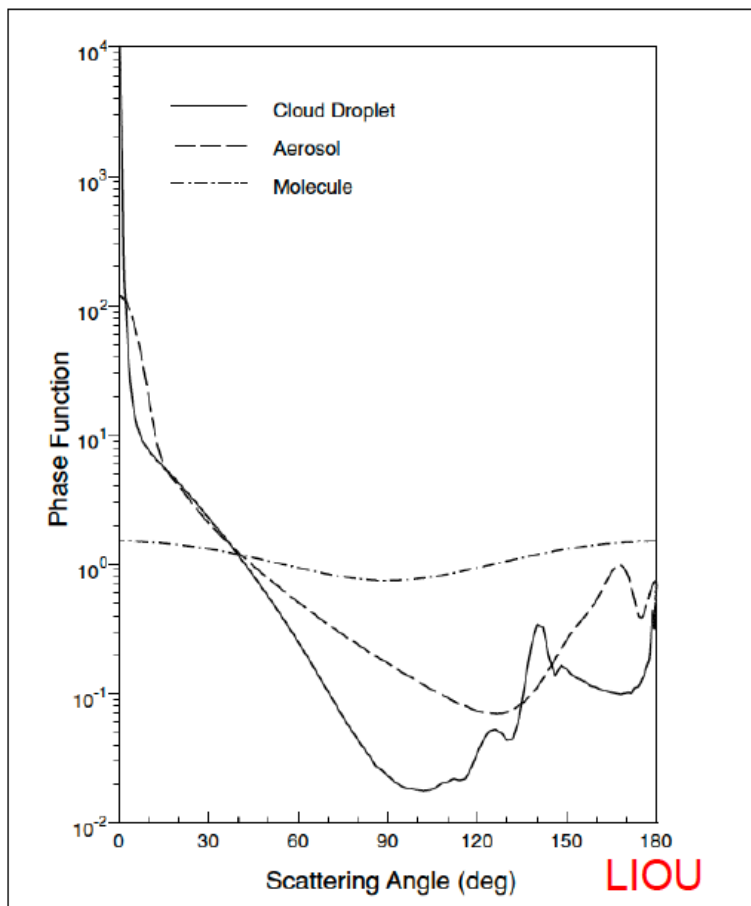


Fig. 8 Scattering of visible light by oil droplets of diameter $0.1 \mu\text{m}$ (solid curve), $0.8 \mu\text{m}$ (dashes), and $10 \mu\text{m}$ (dots)

Craig Bohren



MIE SCATTERING – AROUND A BIGGER SCATTERER



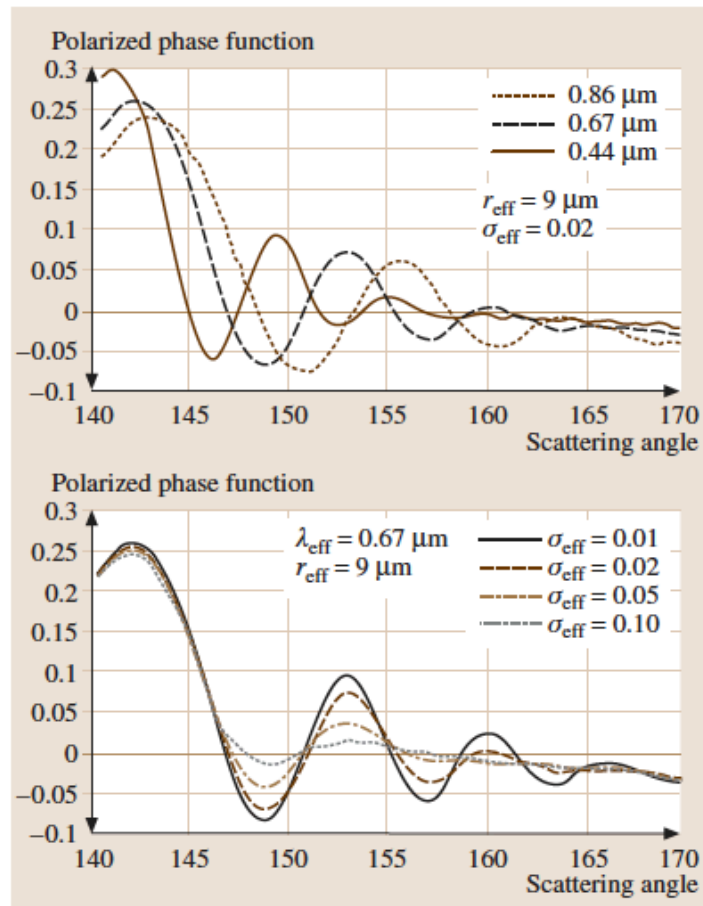
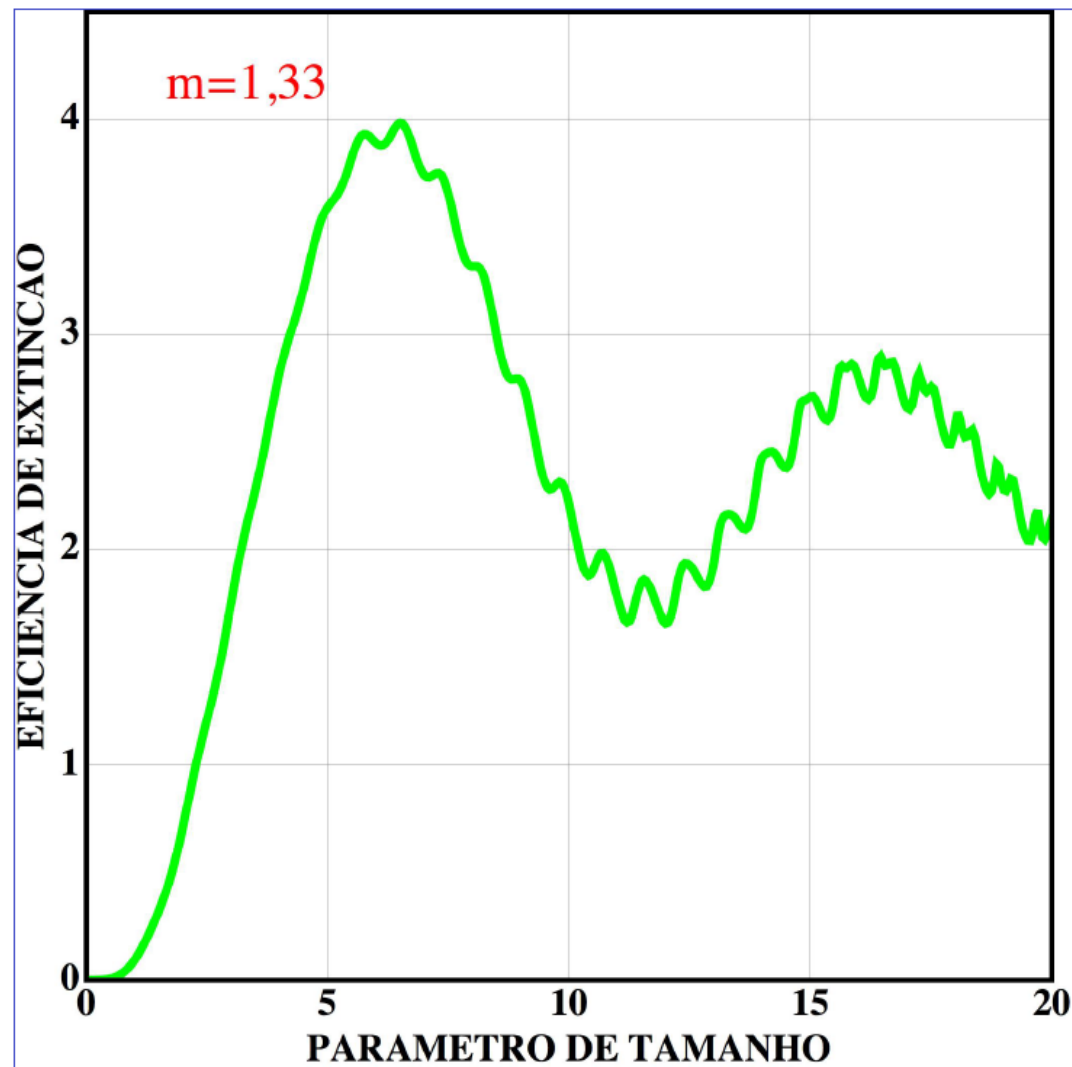
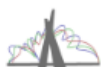
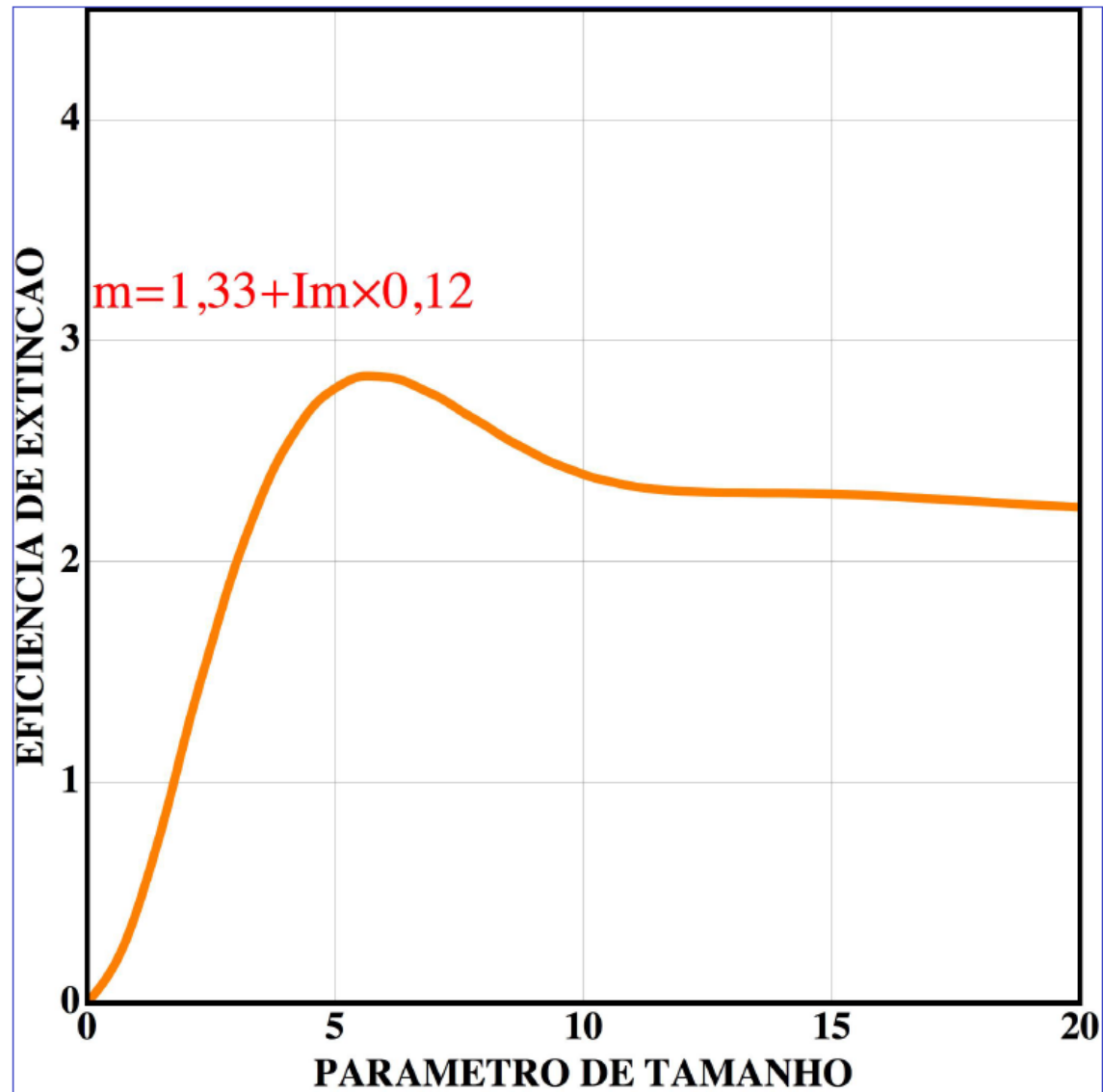


Fig. 19.2 Polarized Mie scattering phase function as a function of scattering angle for cloud droplet having a lognormal particle size distribution with an effective radius $r_{\text{eff}} = 9 \mu\text{m}$. *Upper panel*: phase function as a function of wavelength with fixed $\sigma_{\text{eff}} = 0.02$ effective size variance; *lower panel*: as a function of effective size variance (courtesy of Bréon and Goloub, 2003)

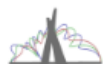
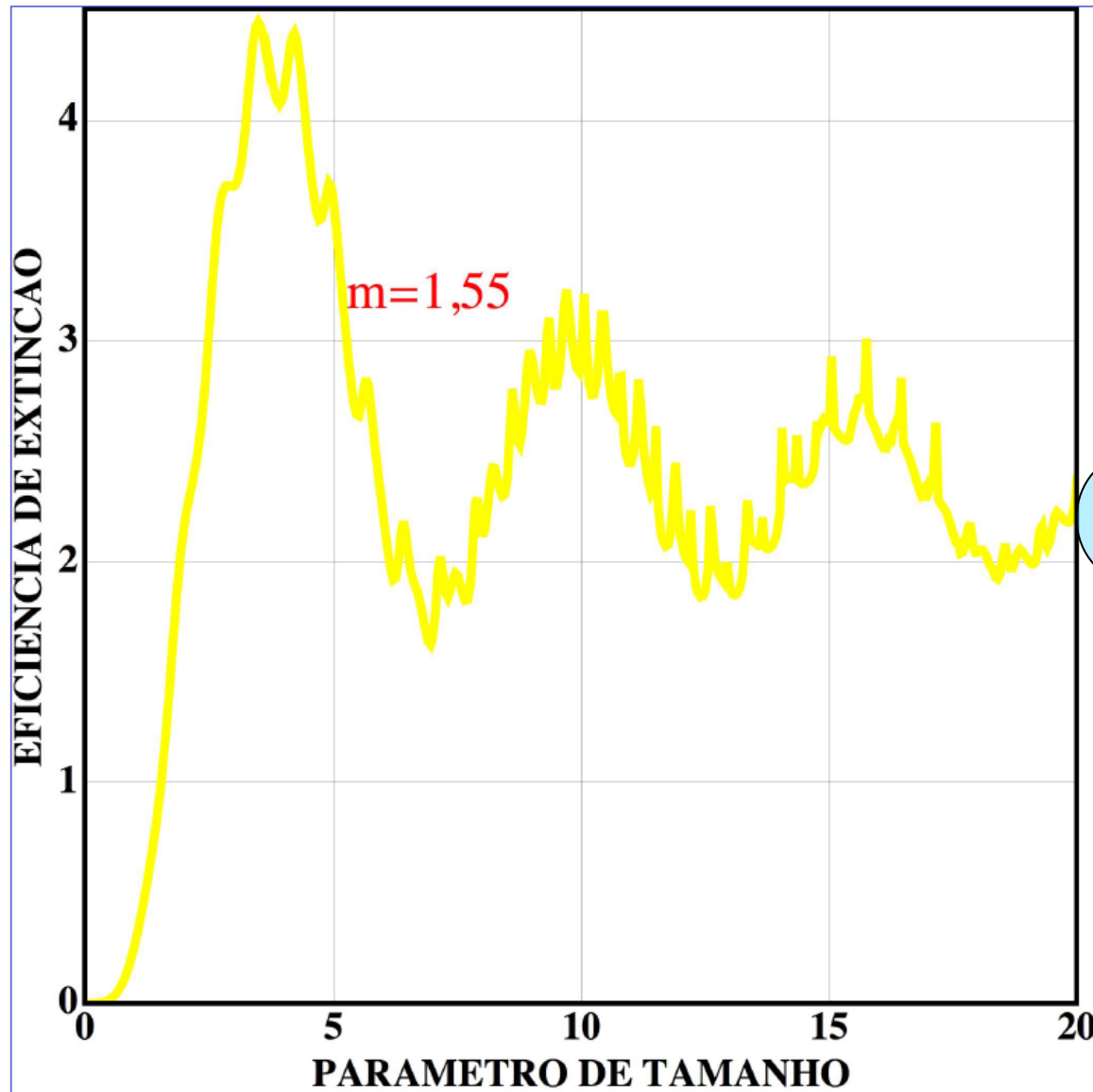
MIE SCATTERING – SOME RESULTS



MIE SCATTERING – SOME RESULTS



MIE SCATTERING – SOME RESULTS



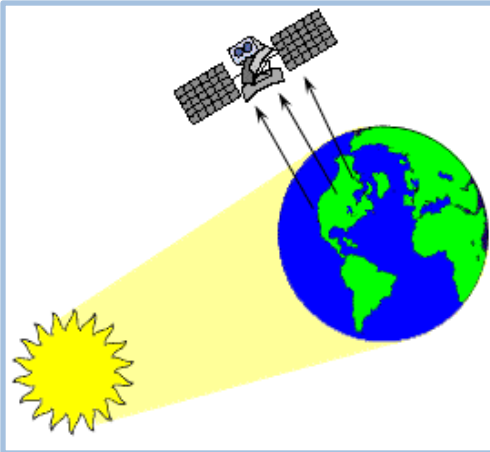
MIE SCATTERING - BUILDING CONCEPTS



WHAT'S THE TYPE OF SCATTERING ???



Passive remote sensing



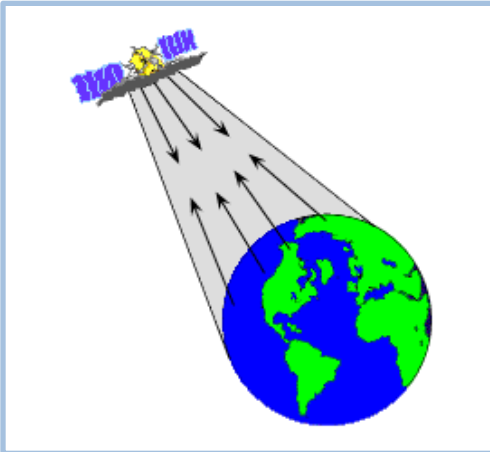
Based on “**uncontrolled illumination**”:

- Sun
- terrestrial emission

Passive methods:

- extinction
- scattering
- longwave emission

Active remote sensing

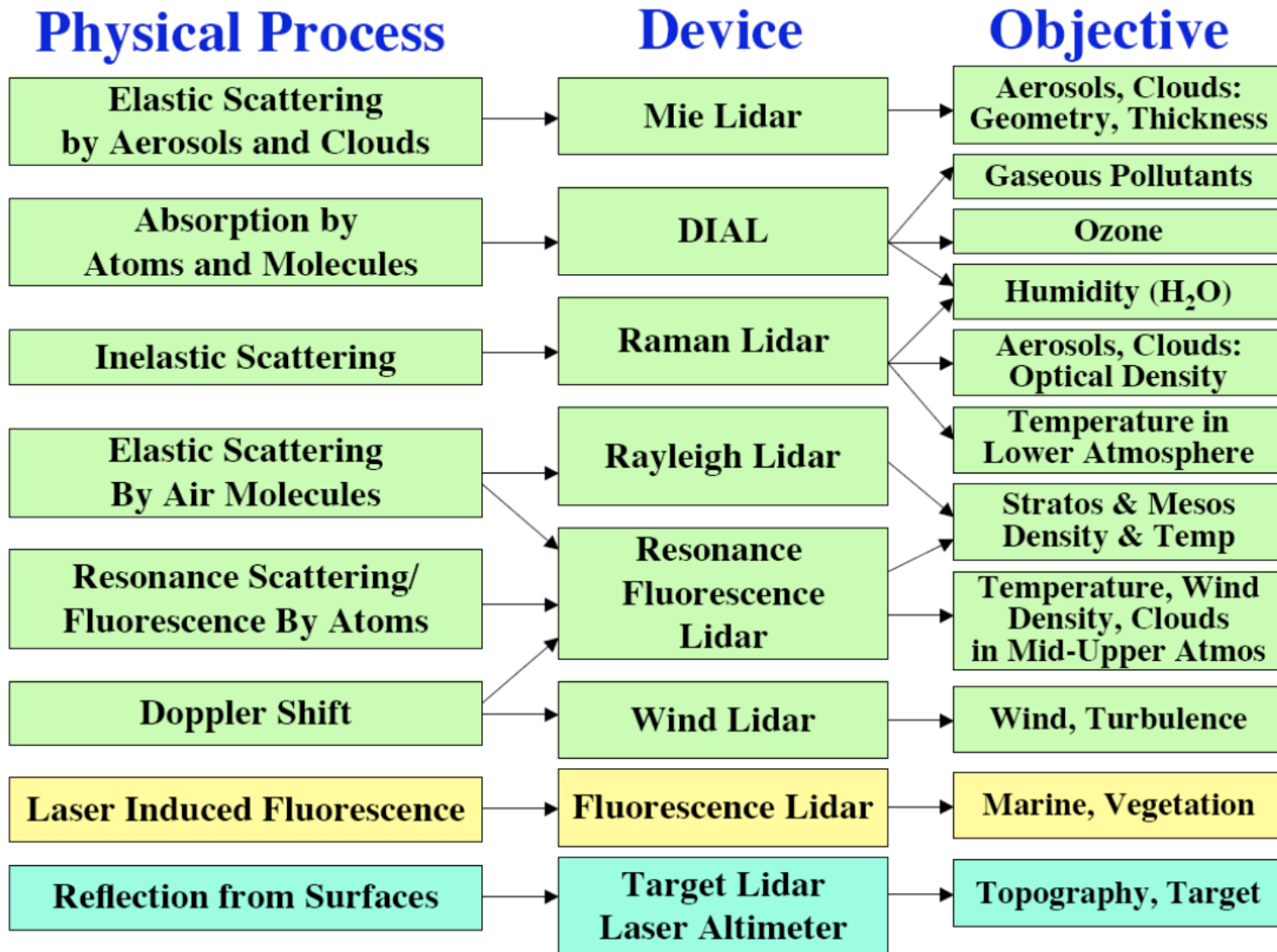


Based on “**controlled illumination**” and measurement of backscattering

Active methods:

- lidar
- radar

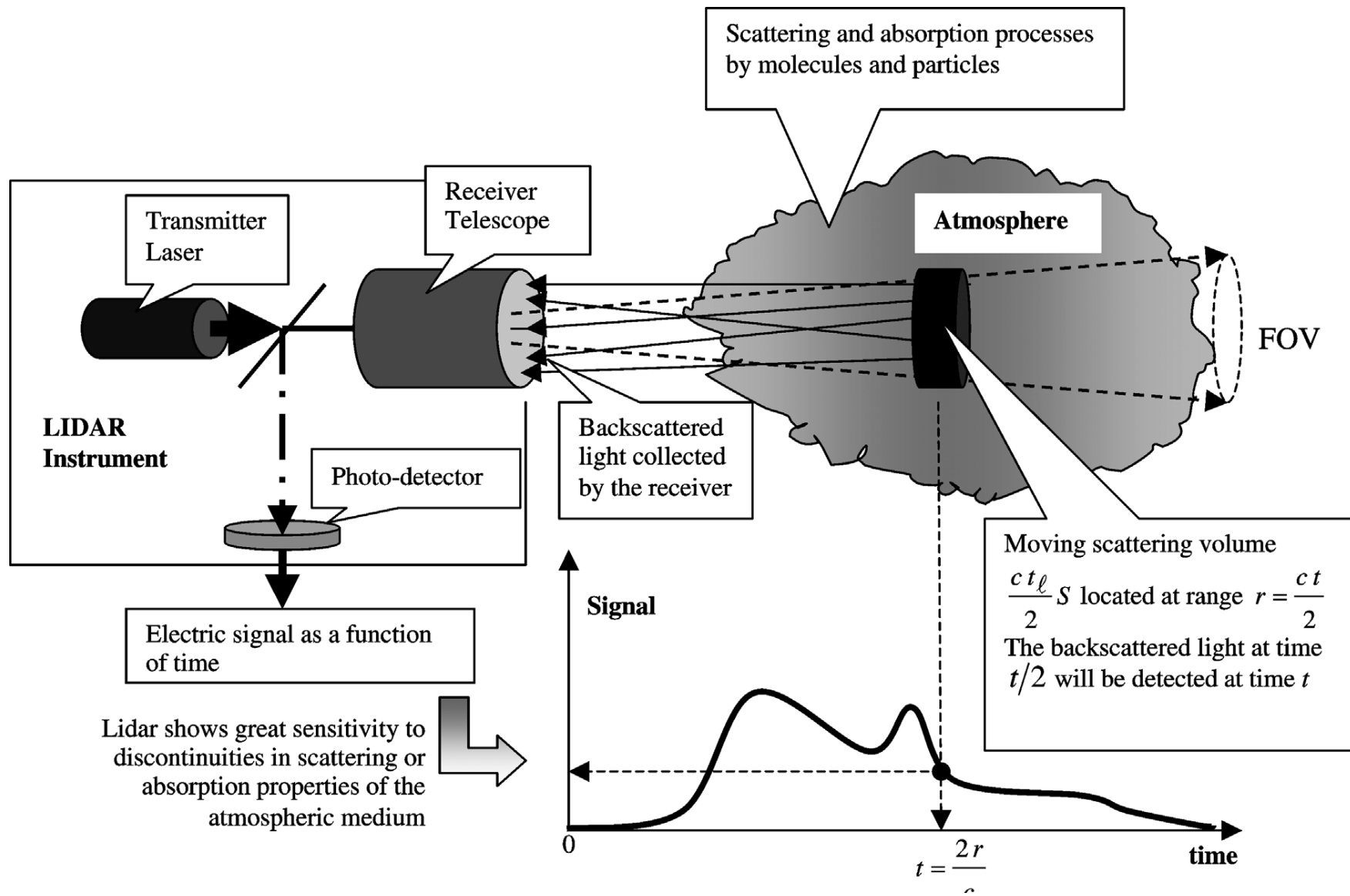
Lidar (light detection and ranging) is an active remote sensing technology that measures distance by illuminating a target with a laser and analyzing the reflected light



Laser-atmosphere interactions...

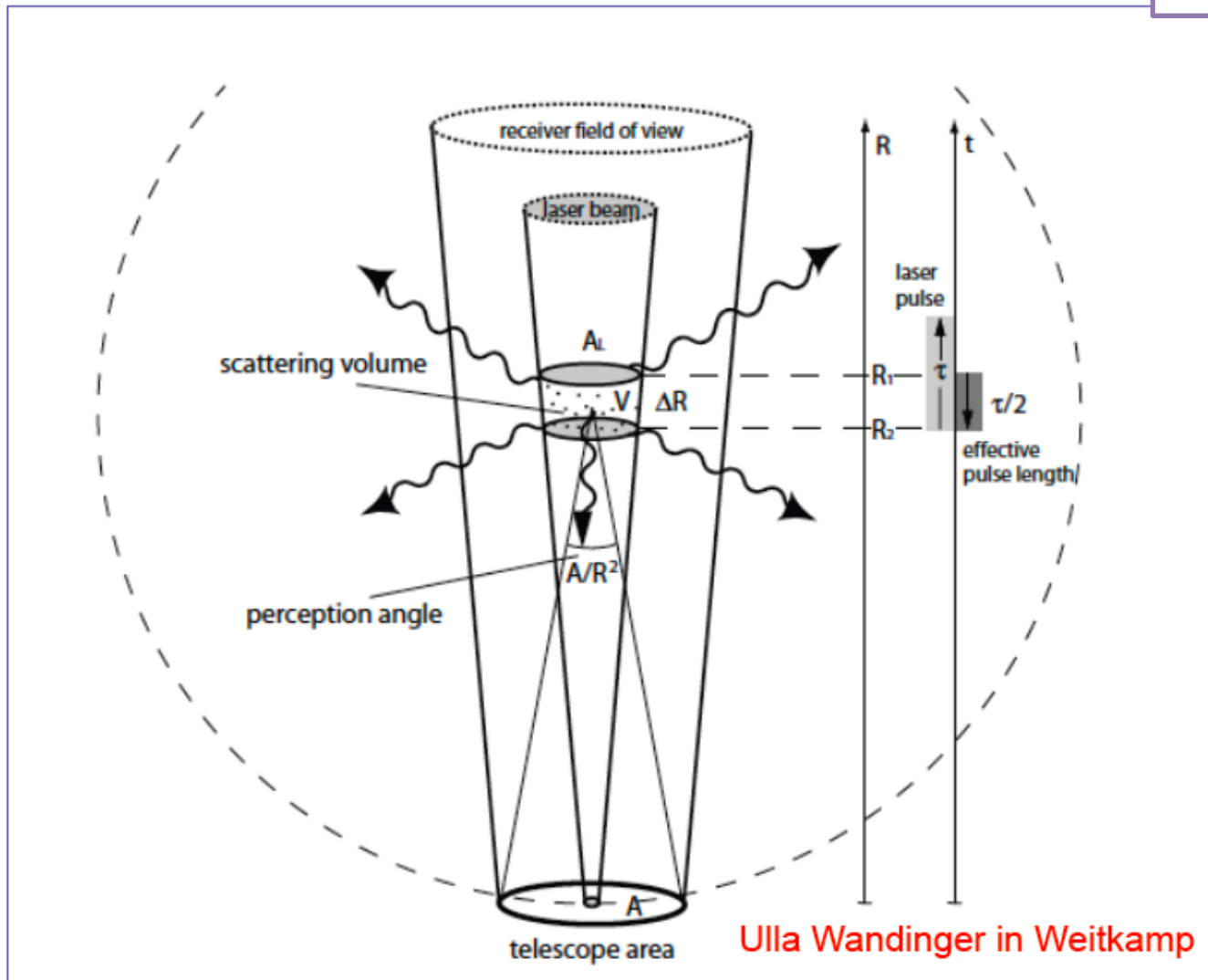
Laser – Atmosphere Interaction	Atmospheric Parameter-Species
Elastic Scattering ($\lambda_1 \equiv \lambda_2$)	Aerosols (PMs), clouds, atmospheric density, atmospheric structure, temperature...
Inelastic Scattering (Raman Scattering) ($\lambda_1 \equiv \lambda_2 + \Delta\lambda_R$)	Water vapor, RH, O ₃ , temperature, Aerosols (extinction, backscatter coefficients)
Differential Absorption DIAL (λ_1, λ_2)	SO ₂ , O ₃ , NO ₂ , NO, CO ₂ , Hg, HF, HCl, NH ₃ , HCs, CO, H ₂ O
Resonance Scattering	K, Na, Li, Ca, Fe
Doppler shift	Wind measurements
Laser Induced Fluorescence (LIF)	OH ⁻





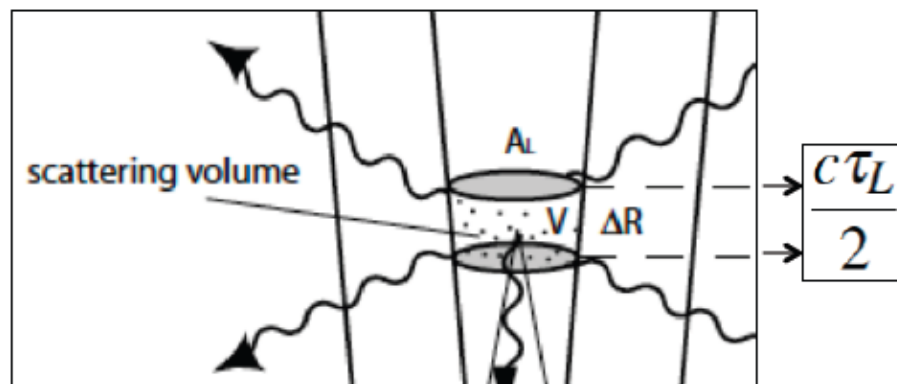
LIDAR EQUATION- BUILDING CONCEPTS

REMOTE SENSING



LIDAR EQUATION – PROBED VOLUME

$$V_P = A_L \cdot \Delta R$$

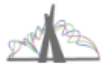
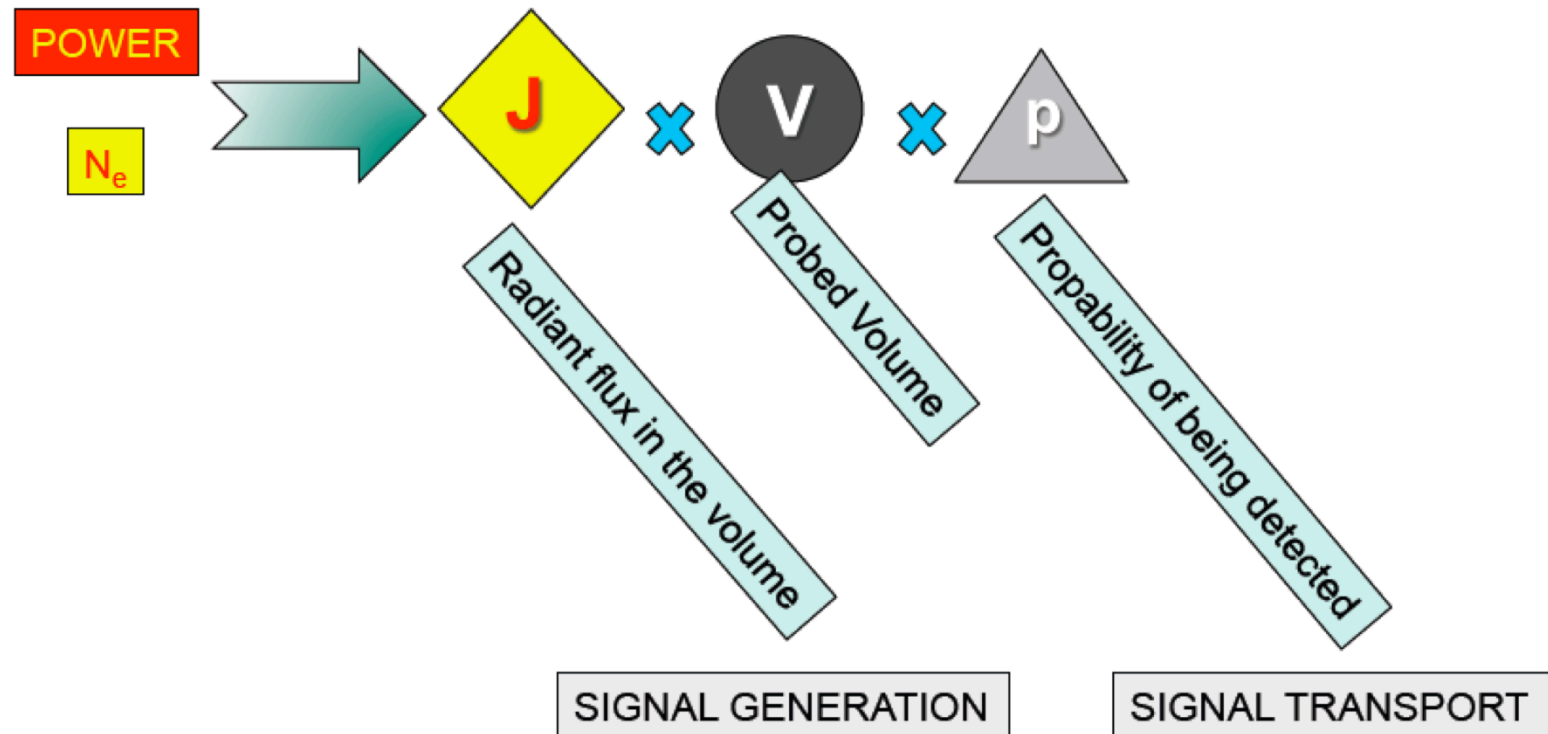


$$V_P = A_L \cdot \frac{c\tau_L}{2}$$



LIDAR EQUATION- BUILDING CONCEPTS

At a given Range (R) and Wavelength (λ) :



LIDAR EQUATION- BUILDING CONCEPTS

REMOTE SENSING

At a given Range (R) and Wavelength (λ) :

SIGNAL GENERATION



SIGNAL TRANSPORT



NATURE OF INTERACTION

INSTRUMENT + ATMOSPHERE

$$J(\lambda, R, r) = \beta_{\pi}(\lambda, R, r) I(R, r)$$

$$p(\lambda, R, r) = \frac{A_0}{R^2} \times T(\lambda, R) \times \epsilon(\lambda) \times \zeta(R, r)$$

- BACKSCATTERING
- IRRADIANCE AT TARGET

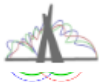
- ATMOSPHERIC TRANSMISSION
- ACCEPTANCE SOLID ANGLE
- SPECTRAL EFFICIENCY
- GEOMETRIC FACTOR



LIDAR EQUATION- TRANSMISSION IN THE ATMOSPHERE

$$T(\lambda, r) \equiv e^{-2 \int_0^R \alpha(\lambda, r) dr}$$

EXTINCTION COEFFICIENT



LIDAR EQUATION – THE FINAL CUT

$$J(\lambda, R, r) = \beta_{\pi}(\lambda, R, r)I(R, r)$$

×

$$V_P = A_L \cdot \frac{c\tau_L}{2}$$

×

$$p(\lambda, R, r) = \frac{A_o}{R^2} \times T(\lambda, R) \times \varepsilon(\lambda) \times \zeta(R, r)$$

$$P_o = I(R, r) \cdot A_L$$

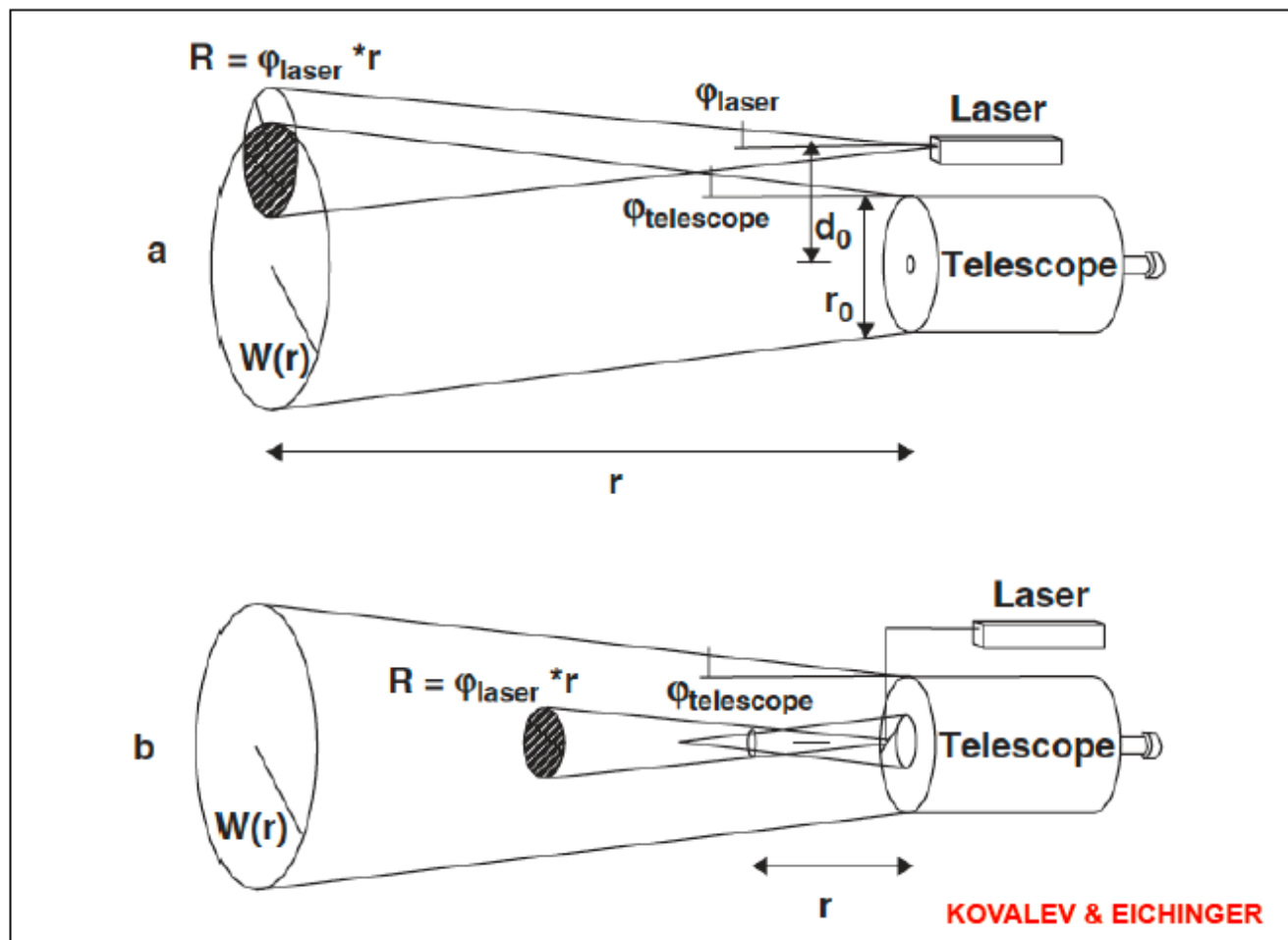
$$T(\lambda, r) \equiv e^{-2 \int_0^R \alpha(\lambda, r) dr}$$

$$P(\lambda, R) = P_o \frac{A_o}{R^2} \beta_{\pi}(\lambda, R) \varepsilon(\lambda) \zeta(R) \cdot \left(\frac{c\tau_L}{2} \right) e^{-2 \int_0^R \alpha(\lambda, r) dR}$$

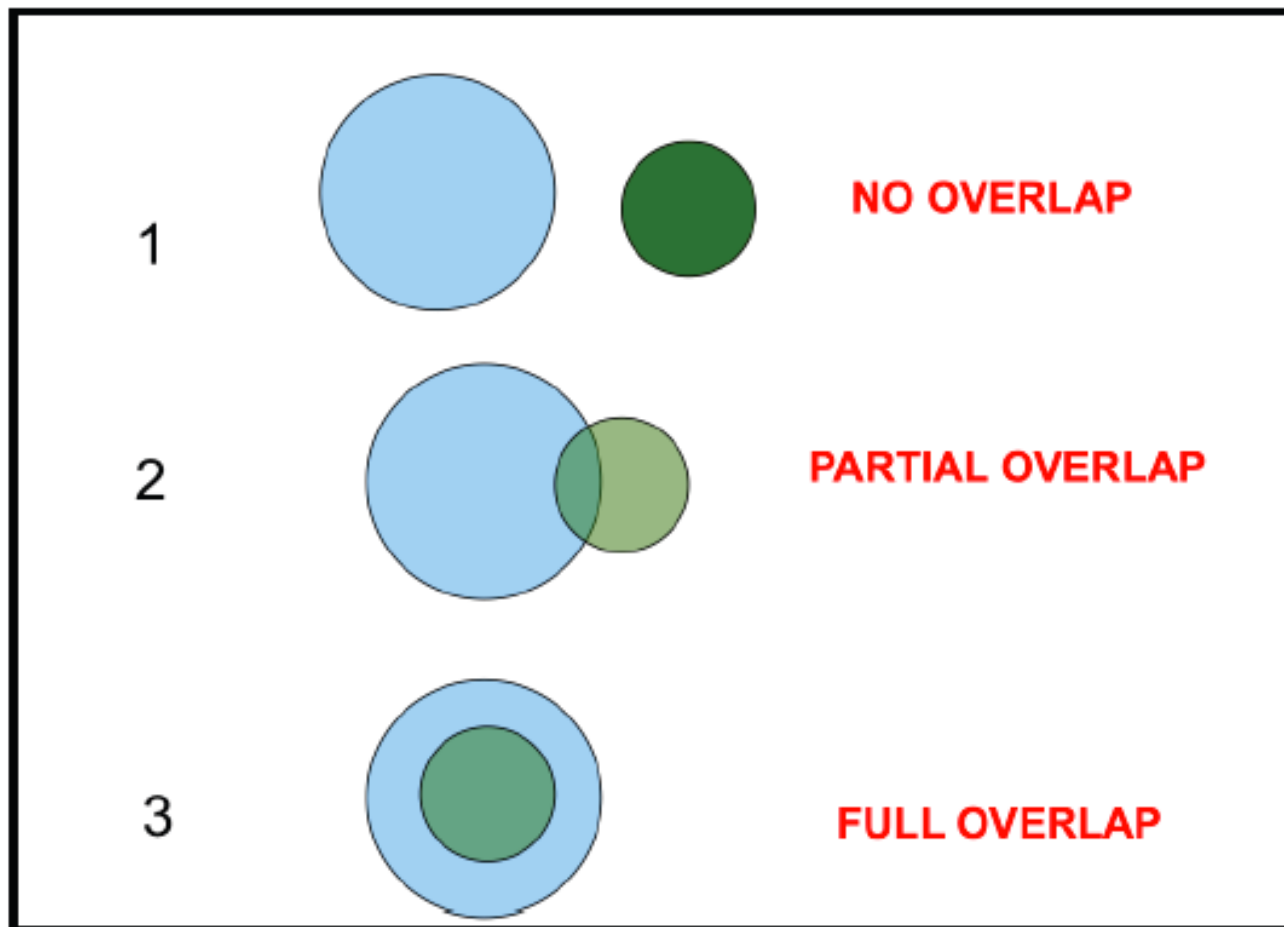
ELASTIC LIDAR EQUATION



LIDAR EQUATION – OVERLAP FUNCTION



LIDAR EQUATION – OVERLAP FUNCTION



LIDAR EQUATION – SOLUTIONS

ATMOSPHERIC OPTICAL PARAMETERS

$$P(\lambda, R) = P_o \frac{A_o}{R^2} \beta_{\pi}(\lambda, R) \varepsilon(\lambda) \zeta(R) \cdot \left(\frac{c\tau_L}{2}\right) e^{-2 \int_0^R \alpha(\lambda, r) dR}$$

BACKSCATTERING COEFFICIENT

$$[\beta(R)] = km^{-1} .sr^{-1}$$

EXTINCTION COEFFICIENT

$$[\alpha(R)] = km^{-1}$$



AEROSOL STUDIES WITH LIDARS – SOLUTIONS

LIDAR RATIO

$$P(\lambda, R) = P_o \frac{A_o}{R^2} \beta_{\pi}(\lambda, R) \varepsilon(\lambda) \zeta(R) \cdot \left(\frac{c\tau_L}{2} \right) e^{-2 \int_0^R \alpha(\lambda, r) dR}$$

$$L_{aer}(R) = \frac{\alpha_{mol}(R)}{\beta_{mol}(R)} = \frac{8\pi}{3} sr$$

LIDAR RATIO (MOLECULAR)

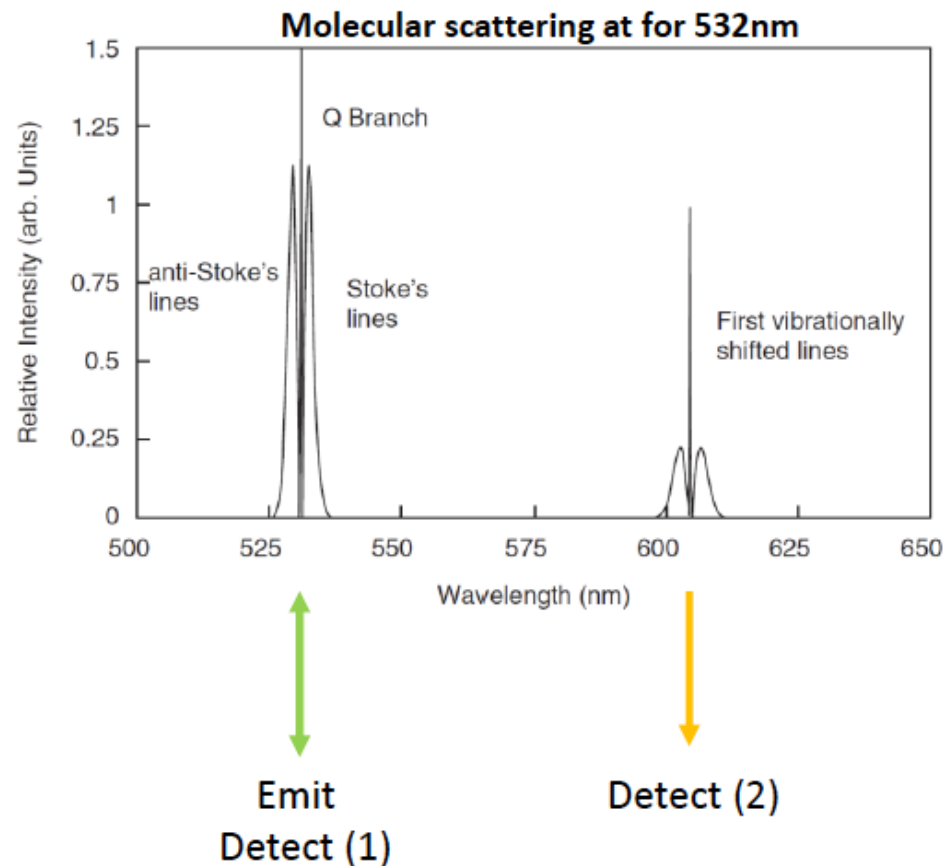
$$L_{aer}(R) = \frac{\alpha_{aer}(R)}{\beta_{aer}(R)}$$

LIDAR RATIO (AEROSOL)



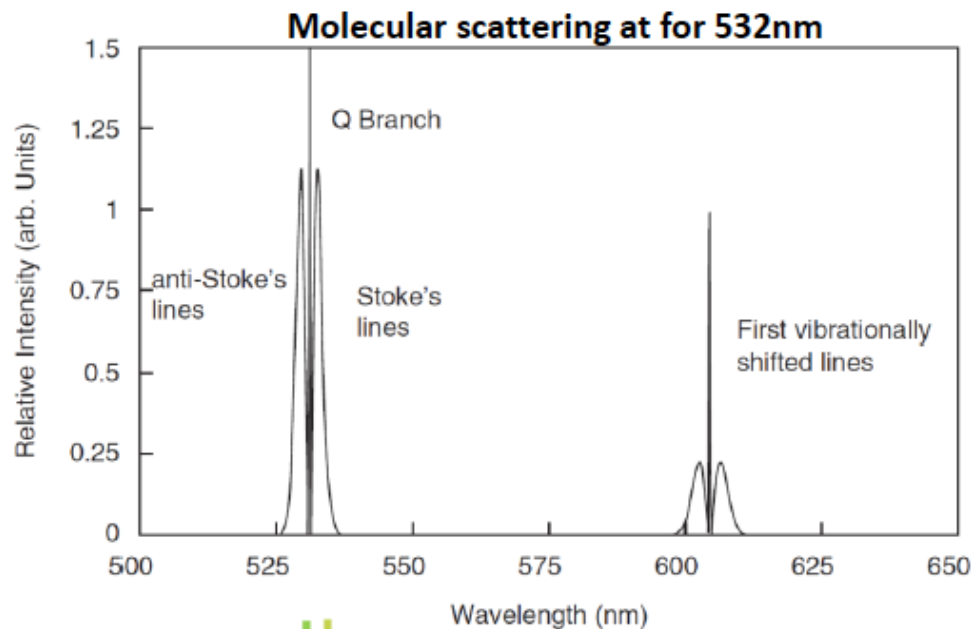
Vibration Raman lidar

- The technique:



Rotational Raman lidar

- The technique:



Emit

Detect (1) Detect (2)



AEROSOL STUDIES WITH LIDARS – RAMAN LIDARS

$$P(\lambda, R) = P_o \frac{A_o}{R^2} \beta_{\pi}(\lambda_L, \lambda_R, R) \epsilon(\lambda) \zeta(R) \cdot \left(\frac{c\tau_L}{2} \right) e^{-\int_0^R \alpha(\lambda_L, r) + \alpha(\lambda_R, r) dR}$$

**RAMAN SCATTERING CROSS SECTION****DIFFERENTIAL TRANSMISSION**

AEROSOL STUDIES WITH LIDARS – RAMAN LIDARS

$$\alpha(355, z) = \frac{\frac{d}{dz} \left[\ln \frac{N(z)}{z^2 P(z)} \right] - \alpha_{mol}(355, z) - \alpha_{mol}(387, z)}{1 + \frac{355}{387}}$$

$\lambda_L = 355 \text{ nm}$

$\lambda_R = 387 \text{ nm}$



**NITROGEN RAMAN
SCATTERING**



$\lambda_L = 355 \text{ nm}$

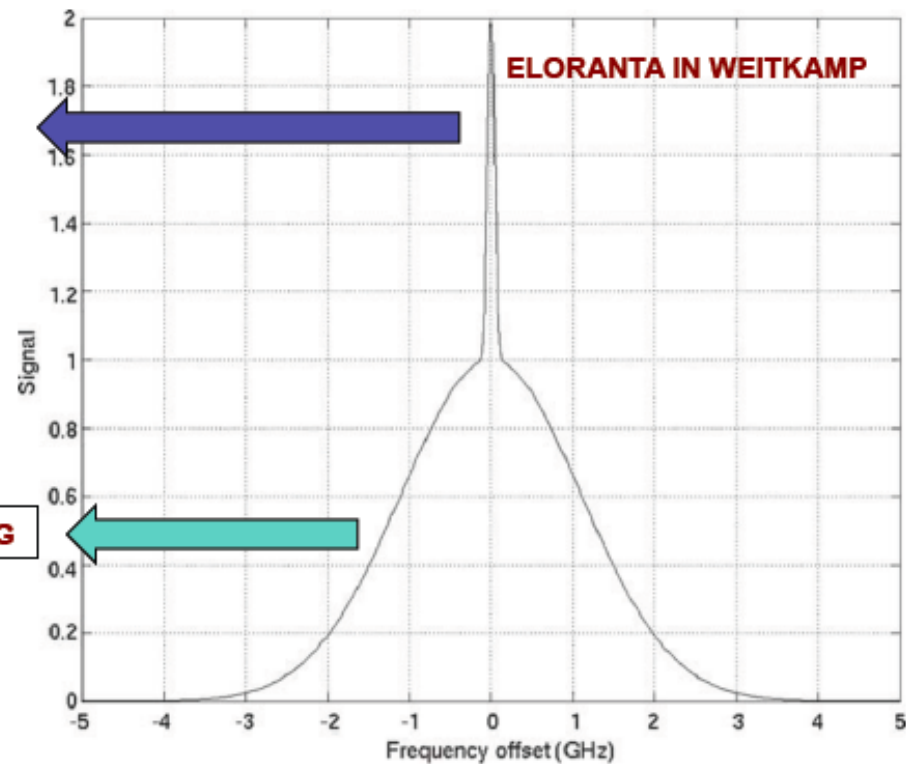


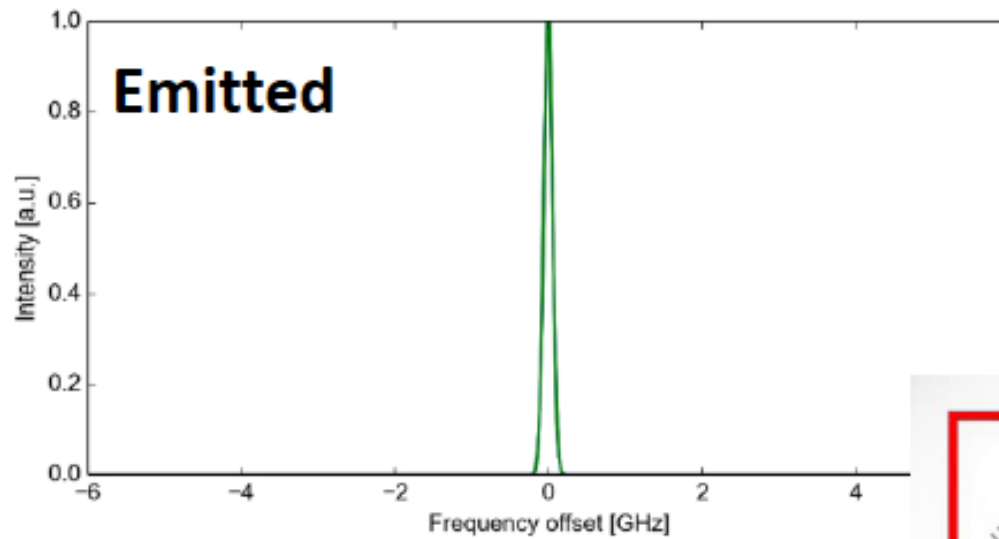
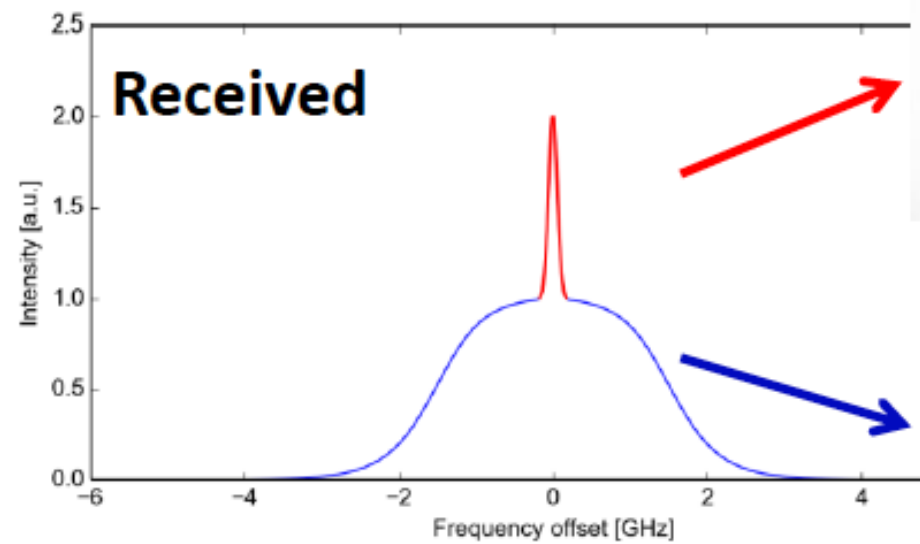
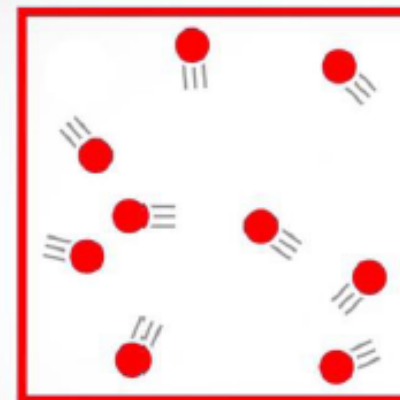
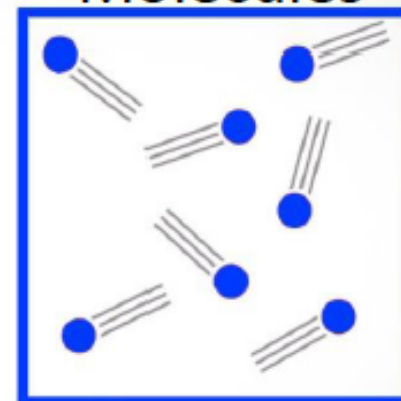
AEROSOL STUDIES WITH LIDARS – HRSL LIDARS

HIGH RESOLUTION SPECTRAL LIDARS

AEROSOL DOPPLER BROADENING

MOLECULAR DOPPLER BROADENING



**Aerosols****Molecules**

AEROSOL STUDIES WITH LIDARS – HRSL LIDARS

HIGH RESOLUTION SPECTRAL LIDARS

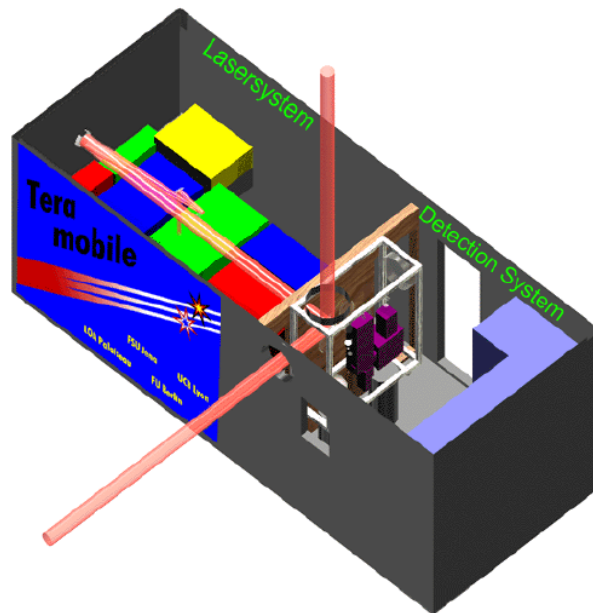
$$P_{\text{mol}}(r) = K_{\text{mol}} r^{-2} O(r) \beta_{\text{mol}}(r) \exp\left(-2 \int_0^r \alpha(r') dr'\right)$$

$$P_{\text{aer}}(r) = K_{\text{aer}} r^{-2} O(r) \beta_{\text{aer}}(r) \exp\left(-2 \int_0^r \alpha(r') dr'\right)$$

$$\mathfrak{R}(r) = \frac{\beta_{\text{aer}}(r)}{\beta_{\text{mol}}(r)} = \frac{K P_{\text{aer}}(r)}{P_{\text{mol}}(r)}$$



Teramobile LIDAR



The TERAMOBILE laser

Laser Parameters :

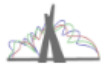
790 nm

350 mJ

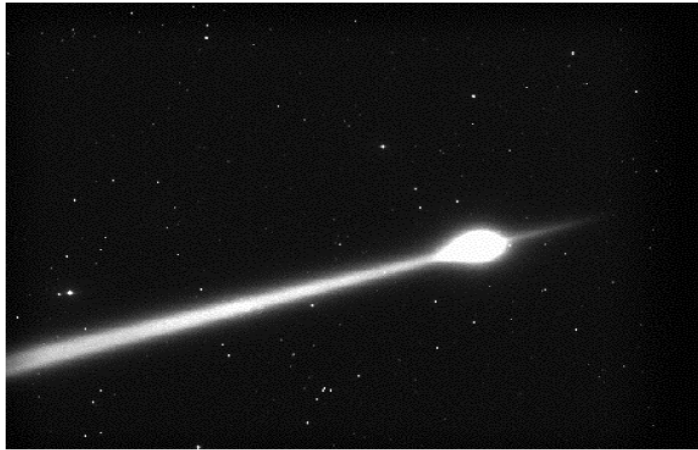
60 fs

5 TW

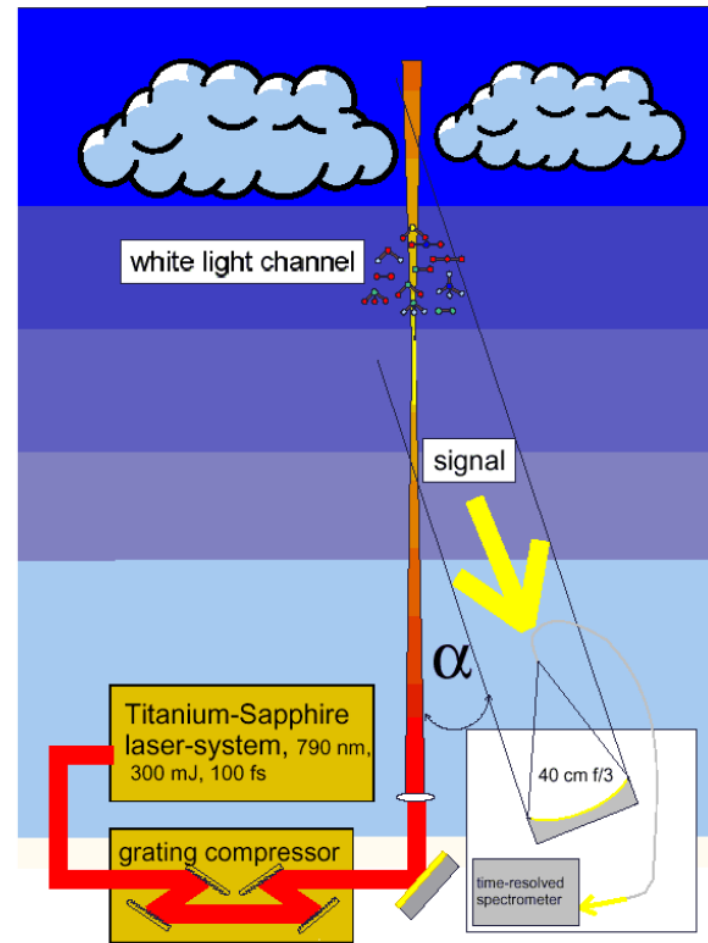
Kasparian J. et al, Science, 301, 61, 2003]



Teramobile LIDAR



Femtosecond lidar



[Kasparian J. et al, Science, 301, 61, 2003]

